NTNU

Norwegian University of
Science and Technology

Wet Gas Compression - IGV Control

Martin Henriksen

Mechanical Engineering
Submission date: June 2017
Supervisor: Lars Eirik Bakken, EPT
Co-supervisor: Levi Andre Berg Vigdal, EPT
Tor Bjørge, EPT
Erik Langørgen, EPT

Norwegian University of Science and Technology
Department of Energy and Process Engineering

NTNU

Norwegian University
of Science and Technology

Department of Energy
and Process Engineering

EPT-M-2017-34

MASTER THESIS

for

Student Martin Henriksen

Spring 2017

Wet Gas Compression – IGV Control

Våtgass Kompresjon – IGV kontroll

Background and objective

Natural gas is one key to reduce emission and optimize efficiency. Increased production of gas demands new field development based on sub-sea production. Several wet gas compressors have been installed subsea at Gullfaks and Åsgard and novel experience from first operating phases is achieved.

Operation of subsea wet gas compressors represents challenges related to performance control and stability. Based on literature review and experiments at the NTNU wet gas compressor test rig it is of interest to document Inlet Guide Vanes (IGV) functionality and impact on performance control. Of specific interest is variation in control capability between dry and wet gas operation.

The following tasks are to be considered:

1. Literature review to document how IGVs are utilize for performance control, and its impact on stability and efficiency.

2. Update current test rig IGV control and by experiments document how the test compressor behave at different IGV control settings in dry gas.

3. Perform and analyse which impact the control settings in section 2) have on wet gas operation. Results should also be compared to the different dry gas test cases.

-- " --

Within 14 days of receiving the written text on the master thesis, the candidate shall submit a research plan for his project to the department.

When the thesis is evaluated, emphasis is put on processing of the results, and that they are presented in tabular and/or graphic form in a clear manner, and that they are analyzed carefully.

The thesis should be formulated as a research report with summary both in English and Norwegian, conclusion, literature references, table of contents etc. During the preparation of the text, the candidate should make an effort to produce a well-structured and easily readable report. In order to ease the evaluation of the thesis, it is important that the cross-references are correct. In the making of the report, strong emphasis should be placed on both a thorough discussion of the results and an orderly presentation.

The candidate is requested to initiate and keep close contact with his/her academic supervisor(s) throughout the working period. The candidate must follow the rules and regulations of NTNU as well as passive directions given by the Department of Energy and Process Engineering.

Risk assessment of the candidate's work shall be carried out according to the department's procedures. The risk assessment must be documented and included as part of the final report. Events related to the candidate's work adversely affecting the health, safety or security, must be documented and included as part of the final report. If the documentation on risk assessment represents a large number of pages, the full version is to be submitted electronically to the supervisor and an excerpt is included in the report.

Pursuant to "Regulations concerning the supplementary provisions to the technology study program/Master of Science" at NTNU §20, the Department reserves the permission to utilize all the results and data for teaching and research purposes as well as in future publications.

The final report is to be submitted digitally in DAIM. An executive summary of the thesis including title, student's name, supervisor's name, year, department name, and NTNU's logo and name, shall be submitted to the department as a separate pdf file. Based on an agreement with the supervisor, the final report and other material and documents may be given to the supervisor in digital format.

☐ Work to be done in lab (Water power lab, Fluids engineering lab, Thermal engineering lab)
☐ Field work

Department of Energy and Process Engineering, 15. January 2017

L E Bakken
Academic Supervisor

Research Advisor:
T. Bjørge
L. Vigdal
E. Langørgen

Preface

The work with this master's thesis have been carried out at the Department of Energy and Process Engineering at the Norwegian University of Science and Technology (NTNU), during the spring of 2017.

I would like to thank my supervisor Lars E. Bakken for guidance, academic discussions and advice throughout the project. I would also like to thank my co-supervisors Levi Andre B. Vigdal for a lot of help, discussions and insight.

Special thanks to to Engineer Erik Langørgen for guidance and assistance in the compressor rig.

Martin Henriksen

Trondheim, 11.06.2017

Abstract

Wet gas compression and subsea technology has gained increased attention in the recent years. Subsea compression increase extraction from aging gas fields and make remote fields profitable. Wet gas compressors eliminate the need for subsea separation, which reduces capital- and operational cost. In turbomachinery, the common practice is to utilize variable inlet guide vanes (VIGV) to manage variations in inlet condition parameters. Stable compressor performance and operation at maximum efficiency point is desirable from both a mechanical and economical point of view. The effect of VIGV on wet gas compression is therefore of specific interest.

A variable inlet guide vanes system has been examined in combination with a single stage centrifugal compressor. The main objective was to assess the influence wet gas has on the VIGV performance, how VIGV performs compared to variable speed drive (VSD) and how the VIGV could be utilized to keep stable compressor performance with varying liquid content. Four different test have been conducted at the NTNU test facility.

VIGV performance has been studied at the following gas mass fractions (GMF); 1.0, 0.98, 0.95, 0.90, 0.80, 0.70 and 0.60. For each of the different values of GMF, the compressor performance was recorded, while the VIGV angle was changed from maximum prewhirl to maximum counter whirl. These experiments resulted in the following findings:

- The VIGV effect on pressure ratio and volume flow declines with increasing liquid content. This is due to the increased momentum transfer between liquid and gaseous phases.
- Increasing liquid content correlated with increased pressure ratio and reduced volume flow. With one exception at GMF 0.98, the pressure ratio and the volume flow increased compared to the dry gas cases.
- The performance of VIGV compared to the performance of VSD differed little with respect to both volume flow and pressure ratio.
- When the VIGV provided counter whirl the overall efficiency of the compressor decreased compared to the VSD controlled compressor case.

To show that the VIGV could be used to keep stable compressor performance with varying liquid content, the inlet composition was changed from dry gas to the following GMF; 0.9, 0.8 and 0.7. The VIGV and the outlet valve were used to keep the same pressure ratio and volume flow independent of liquid content. For GMF 0.9 and GMF 0.8 the VIGV was used to lower the compressor performance by inducing prewhirl. While for GMF 0.7 the compressor performance was increased by inducing less prewhirl. The maximum change in VIGV angle needed was 3.5°.

Utilization of VIGV was demonstrated as an efficient method to adjust the compressor performance with varying inlet liquid conditions, even though the VIGV effect on pressure ratio and volume flow decreased with increasing liquid content.

Sammendrag

Fokuset på våtgasskompresjon og subseateknologi har økt de siste årene. Subseakompresjon kan øke produksjonen av aldrende gassfelt samt gjøre tidligere utilgjengelige felt lønnsomme. For å håndtere varierende innløpsforhold er det vanlig å ta i bruk justerbare innløpsledeskovler (VIGV). Både mekanisk og økonomisk er det ønskelig med stabil kompressorytelse samt drifte på høyest mulig virkningsgrad under drift. Hvordan VIGV påvirker våtgasskompresjon er derfor av spesiell interesse.

En VIGV-konfigurasjon har blitt undersøkt i kombinasjon med en ett-stegs sentrifugalkompressor. Hovedfokuset var å vurdere påvirkningen våtgass hadde på VIGV-ytelsen, hvordan VIGV presterer i forhold til variabler hastighets kontroll VSD og hvordan VIGV kan brukes til å holde stabil kompressorytelse selv ved varierende væskeinnhold. Fire ulike tester er blitt gjennomført på testfasilitetene ved NTNU.

VIGV-ytelsen har blitt studert ved følgende massefraksjoner (GMF); 1.0, 0.98, 0.95, 0.90, 0.80, 0.70 og 0.60. For hver av disse gassmassefraksjonene ble kompressorytelsen logget, mens VIGV-vinkelen ble justert fra maksimum medrotasjon til maksimum motrotasjon. Disse eksperimentene ga følgende funn:

- Effekten VIGV har på trykkforhold og volumstrøm minker med økende væskeinnhold. Dette kan forklares med økt bevegelsesmengde mellom væske- og gassfasene.
- Økt væskeinnhold korrelerte med økt trykk forhold og redusert volumstrøm. Med et unntak på GMF 0.98, trykkforholdet og volumstrømmen økte sammenlignet med tørr gass.
- Væskeinnholdet påvirker kompressorytelsen og fører til økt trykkforhold og redusert volumstrøm. Unntaket er ved GMF 0.98, ved denne væskemengden øker trykkforholdet og volumstrøm.
- Ytelsen til VIGV sammenlignet med VSD varierte med hensyn på til trykkforhold og volumstrøm.
- Når VIGV ga medrotasjon sank den overordnede effektiviteten til kompressoren sammenlignet med VSD.

For å vise at VIGV kan bli brukt til å beholde kompressorytelsen konstant ved varierende væskemengde, ble innløpskomposisjonen endret i fra tørr gass til følgende GMF; 0.9, 0.8 og 0.7. VIGV og utløpsventilen ble brukt til å holde trykkforholdet og volumstrømmen konstant ved forskjellige væskeinnhold. For GMF 0.9 og 0.8 ble VIGV brukt til å senke kompressorytelsen ved å gi økt motrotasjon. Med for GMF 0.7 ble kompressorytelsen økt ved å gi mindre motrotasjon. Den største endringen i VIGV-vinkel var 3.5°.

VIGV har vist seg å være et raskt og verdifullt instrument til å justere kompressorytelsen når væskeinnholdet varierer, til tross for at VIGV-effekten på trykkforhold og volumstrøm minsker når væskeinnholdet øker.

Table of content

List of figures

List of tables

Nomenclature

Latin letters		
a	Speed of sound	m/s
C	Absolute velocity	m/s
c	Cord length	mm
D	Diameter	m
E	Elasticity	[-]
f_s	Schultz correction factor	[-]
H	Head	J/kg
h	Specific enthalpy, Head	J/kg
i	Incidence angle	°
m	Mass	kg
$\dot{m}$	Mass flow	kg/s
Ma	Mach number	[-]
Mu	Peripheral Mach Number	[-]
n	Polytropic exponent	[-]
n_T	Polytropic temperature exponent	[-]
n_V	Polytropic volume exponent	[-]
p	Static pressure	Bar
$\dot{Q}$	Volume flow	m^3/s
$\widehat{Q}$	Relative VIGV effect on volume flow	[-]
R	Gas constant	J/kg K
r	Radius	Mm
Re	Reynolds number	[-]
s	Pitch (or space)	Mm
St	Stokes number	[-]
t	Thickness	[-]
T	Temperature	K, C
u, U	Impeller velocity	m/s
V	Relative velocity	m/s
v	Specific volume	m^3/kg
w	Work per unit mass	J/kg
We	Weber number	[-]
X	Compressibility function	[-]
Y	Compressibility function, Expansion factor	[-]
Z	Compressibility factor	[-]
Greek letters		
α	Gas volume fraction,	[-]
α	Absolute velocity angle	°
α'	Blade angle	°
β	Gas mas fraction	[-]
β	Relative velocity angle	°
β_s	Stagger angle	°
γ	Viscosity ratio	[-]
δ	Density ratio	[-]
δ	Deviation angle	°
ε	Deflection angle	°
θ	Camber angle	°
ζ	Loss coefficient	[-]

η_p	Polytropic efficiency	[-]
κ	Isentropic exponent, specific heat ratio	[-]
μ	Dynamic viscosity	pa s
ν	Kinematic viscosity	m^2/s
ρ	Density	kg/m^3
π	Pressure ratio	[-]
$\hat{\pi}$	Relative VIGV effect on pressure ratio	[-]
σ	Surface tension	N/m
τ	Droplet relaxation time	s
ω	Angular velocity	1/s

Subscripts	
0	Characteristic length, inlet IGV
1	Inlet impeller
2	Outlet impeller
a	Axial direction
d	Droplet, design, dry
e	Impeller
g	Gas
Imp	Impeller
L, l	Liquid
m	Mixture
mp	Multiphase
p	Polytropic
r	Radial direction
rel	Relative
s	Isentropic
S	Schultz
tot	Total
w	Tangential direction

Abbreviations	
ASME	The American Society of Mechanical Engineers
FT	Flow Transmitter
GMF	Gas mass fraction
GVF	Gas volume fraction
HT	Humidity Transmitter
IGV	Inlet guide vanes
ISO	The International Organization for Standardization
LVF	Liquid volume fraction
MEG	Ethylene glycol
NF	Fan nozzle
NGL	Natural gas liquids
PMMA	Poly(methyl methacrylate)
PT	Pressure Transmitter
TM	Torque Transmitter
TT	Temperature Transmitter
VIGV	Variable inlet guide vanes
VSD	Variable speed drive

1. Introduction

The Norwegian oil production peaked in 2001 and is expected to decrease in the upcoming years [1]. However, the total petroleum production quantity is still at high level due to increased gas production, as seen in Figure 1.1. This growth makes natural gas a more important element in the Norwegian petroleum industry and the attention has in the recent years shifted to some large gas and condensate fields and some smaller and more remote discoveries.

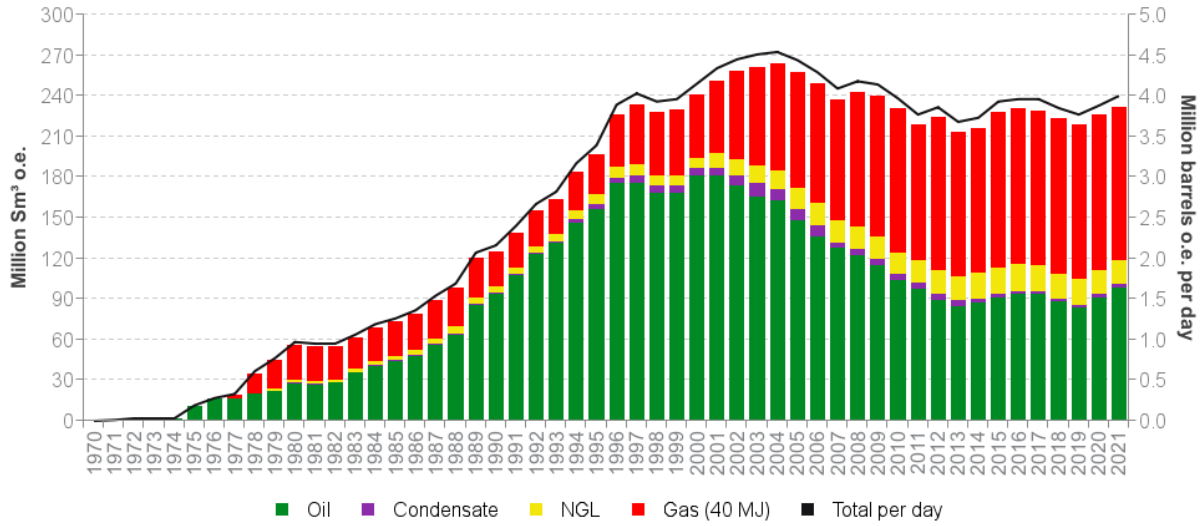

Figure 1.1: Norwegian oil and gas production [1].

Subsea boosting involves compressing and pressurising untreated oil and gas at the seabed. This enables exploitation of small discoveries and fields with low wellhead pressure. In addition extend the lifetime of existing oil and gas fields. However, the technology is challenging. Untreated natural gas contains liquid condensate, which has an extensive effect on compressor performance. This leads to the origin of the term “wet gas compression”. A wet gas compressor is a subsea booster able to compress a mixture of gas and liquid, containing down to 95% gas per volume fraction [2]. An essential advantage of the wet gas compressor is that it eliminates the need for subsea separation.

Variable inlet conditions are not uncommon for turbomachinery, changes may be alterations in temperature, pressure and composition. This will result in a shift in performance and off-design operation. To manage these changes, the common practise is to use variable inlet guide vanes. They can either effect the operational range or have the same impact as changing engine speed. Stable compressor performance and operating at best efficiency point is desirable from the mechanical and economical point of view. The effect VIGV is therefore of specific interest.

Statoil ASA has been a key driving force to develop and test wet gas compression. The company have now subsea compressors at two different fields, Gullfaks and Aasgard. The Gullfaks compressor receives flow directly from the well, while Aasgard is equipped with a separator upstream a liquid tolerant compressor.

NTNU and Statoil have collaborated since 2006 on a research programme regarding the influence of wet gas in centrifugal compressors. The test facility consists of an open loop, single stage centrifugal compressor operating at a low pressure ratio and the test fluids are air and water.

The experimental results later presented in this report are obtained from this test facility.

1.1 Problem description

Variable inlet guide vanes have the ability to change and optimize the compressor performance, and have a positive effect on aerodynamic instabilities. The IGV impact on dry gas is well documented while knowledge on how it performs with wet gas is limited.

The tasks for this report can be summarized as the following:

1. Literature review to document how IGVs are utilize for performance control, and its impact on stability an efficiency.
2. Update current test rig IGV control and by experiments document how the test compressor behave at different IGV control settings in dry gas.
3. Perform and analyse which impact control the control settings in section 2) have on wet gas operation. Results should be compared to the different dry gas test cases.

Risk assessment are included in Appendix A.

Limitations

Analysing the performance of variable inlet guide vanes in wet gas compression is a complex assignment. To narrow the scope, the main focus has been on how changing the VIGV settings affect the compressor performance with respect to pressure ratio and volume flow.

Comments

Sections in Chapter 2 and Chapter 3 are taken from the author project work [3].

1.2 Report structure

Chapter 2: An introduction of the basic theory for centrifugal compressors, wet gas, dimensionless parameters and compressor characteristics. Emphasis has been put on how the centrifugal compressor reacts to wet gas.

Chapter 3: Presentation of the basic theory for inlet guide vanes. The aerodynamical behaviour is explained and how wet gas affects the flow is discussed. IGV impact on stability and surge is presented.

Chapter 4: Description of the NTNU test facility. Emphasis has been put on the VIGV assembly.

Chapter 5: Presentation of the experimental procedure, with anticipated results.

Chapter 6: Presentation and evaluation of the results.

Chapter 7: Conclusion of the rapport including further work.

2. Wet gas compression theory

This report will focus on centrifugal compressors, as that is the focus of most the industry for subsea compression. In addition, the NTNU test facility is equipped with a single stage centrifugal compressor.

The aim of this chapter is to give a brief introduction on how a centrifugal compressor works, the fundamentals of wet gas, dimensionless parameters and how the compressor is affected by wet gas. A more thorough review is presented in the authors project work [3].

2.1 Principle of operation

This section presents the principles of operation for a centrifugal compressor. The theory in this chapter is primarily based on Saravanamutto et. al. [4].

The centrifugal compressor consists of a stationary casing containing a rotary impeller and a diffuser. The impeller increases the static pressure and the kinetic energy of the flow, while the diffuser decelerates the flow and raises the static pressure. A compressor is often designed to have the same velocity out of the diffuser as it has into the impeller, implying a net pressure gain. The standard design of centrifugal compressors aims to make about half the pressure rise in the impeller, while the other half is raised in the diffuser. Figure 2.1 is a diagrammatic sketch of a centrifugal compressor presenting the main parts.

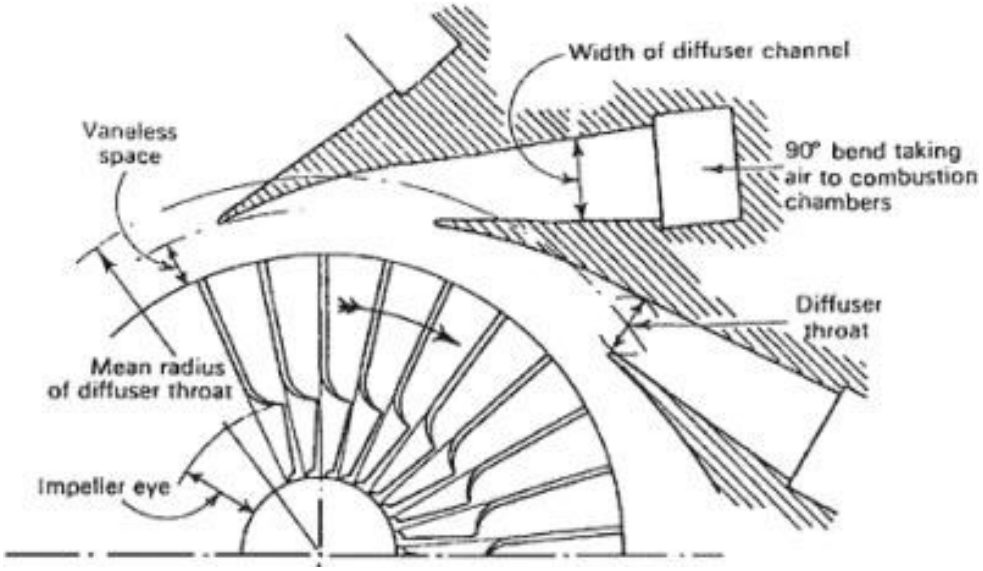

Figure 2.1: Sketch of a centrifugal compressor [4].

The impeller will solely determine the energy of the flow leaving the compressor, as no work is done by the diffuser. The flow enters the compressor with a velocity C_1 and the impeller rotates with a velocity U_e, combining these gives a relative velocity V_1 at an angle α. When there is no prewhirl at the inlet, the absolute inlet velocity C_1 equals the axial velocity C_{a1}. The flow leaves the impeller tip with an absolute velocity C_2, with a tangential component C_{w2} and a radial component C_{r2} . Figure 2.2 shows two velocity triangles, one at ideal conditions $C_{w2} = U$ and one real with $C_{w2} < U$.

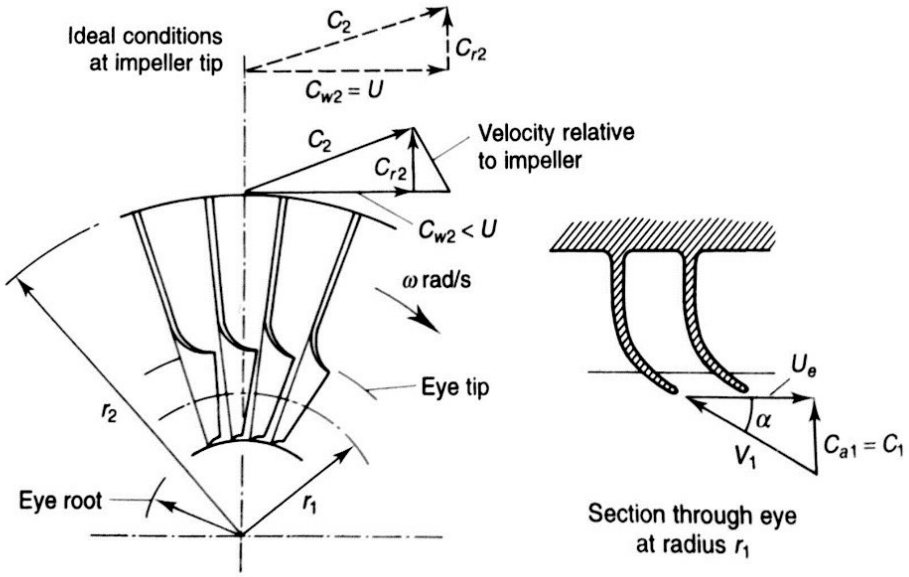

Figure 2.2: Inlet and outlet velocities from the impeller [4].

The change of angular momentum experienced by the flow equals the work done by the impeller. The work per unit mass is expressed in Equation 2.1, where ω is the angular velocity and r is the radius.

$$w = \omega(C_{w2}r_2 - C_{w1}r_1) \tag{2.1}$$

If the centrifugal compressor has an axial inlet, similar to no prewhirl induced by IGVs, C_{w2} is zero and the equation reduces to:

$$w = \omega(C_{w2}r_2) \tag{2.2}$$

When it comes to wet gas compression, there are uncertainties regarding design and performance calculation. Being able to adjust the performance is therefore desirable. This could be done by VIGV or VSD, which enables control of the C_{w1} component or the angular velocity, respectively. Changing the engine speed affects the u component, which affects the angular velocity, as seen in Equation 2.3.

$$\omega = {}^{u}/_{r} \tag{2.3}$$

When increasing the liquid content, Hundseid [5] estimates that the tangential component C_{w2} increases for backswept impellers due to the conservation of mass. Backswept impellers have curved vanes that gives increased relative velocity V_2 and reduced absolute velocity C_2, this leads to increased efficiency for both impeller and diffuser due to less stringent diffusion requirements. The change in velocity diagram is displayed in Figure 2.3, where subscript mp stands for multiphase and d for dry gas.

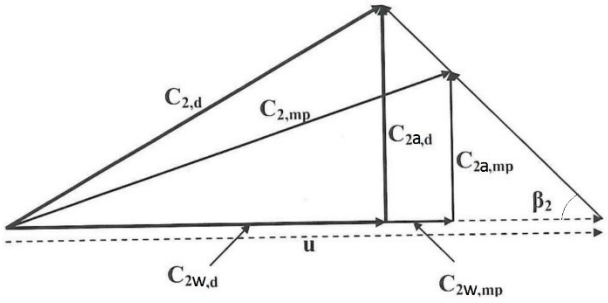

Figure 2.3: Theoretical outlet velocity triangle, for dry and multiphase flow [5].

2.2 Thermodynamics

This chapter aims to present the thermodynamic approach to calculate compressor performance. An accurate calculation is essential to estimate real gas performance parameters, this applies for both the isentropic and polytropic approach. The compression processes are presented in Figure 2.4. This chapter will only present Schultz method. The theory in this chapter is primarily based on Bakken [6] and Schultz [7].

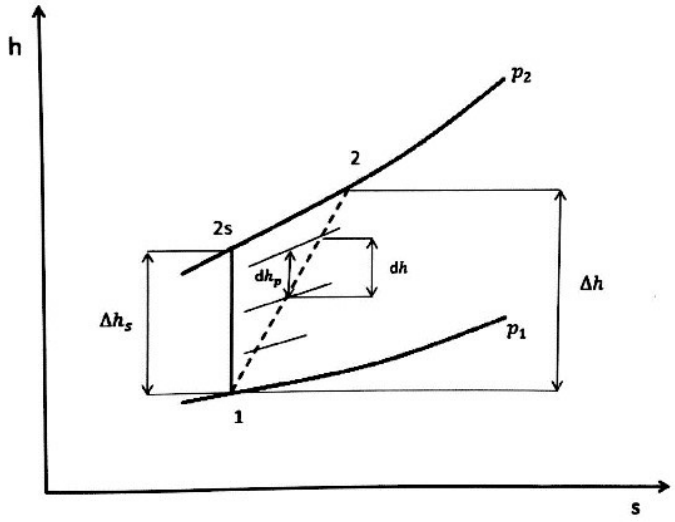

Figure 2.4: Enthalpy versus entropy diagram for isentropic and polytropic compression [6].

2.2.1 Schultz method

In 1962, John M. Schultz improved the accuracy of the polytropic approach by introducing two additional compressibility factors, X and Y:

$$X = \frac{T}{v}\left(\frac{\partial v}{\partial p}\right)_p - 1 \tag{2.4}$$

$$Y = -\frac{p}{v}\left(\frac{\partial v}{\partial p}\right)_T \tag{2.5}$$

Furthermore, Schultz described how the polytropic volume and temperature exponents are based on the compressibility functions:

$$n_v = \frac{1+X}{Y\left[\frac{1}{\kappa}\left(\frac{1}{\eta_p}+X\right)-\left(\frac{1}{\eta_p}-\right)\right]} \tag{2.6}$$

$$\frac{n_T-1}{n_T} = \frac{\kappa-1}{\kappa}\frac{\left(\frac{1}{n_p}+X\right)Y}{(1+X^2)} \tag{2.7}$$

To consider the polytropic volume exponent, n_v, to be constant throughout the compression process is reasonable. Schultz however, accommodated for the slight variations along the compression path by introducing a correction factor, f_s. By Schultz approach the head is described as:

$$\Delta h_{p,s} \cong f_s \frac{n_v}{n_v-1} Z_1 R T_1 \left[\left(\frac{p_2}{p_1}\right)^{\frac{n_v-1}{n_v}} - 1\right] \tag{2.8}$$

Where:

$$f_s = \frac{h_{2s}-h_1}{\frac{\kappa_v}{\kappa_v-1}(p_2 v_{2s} - p_1 v_1)} \tag{2.9}$$

Both ASME and ISO standard for compressor analysis are based on the Schultz polytropic approach [5].

2.2.2 Wet gas thermodynamics

At present, no standard review method exists for performance evaluation of wet gas compression. However, there are two different wet gas performance models, a two-fluid model and a total fluid model.

The two-fluid approach assumes that the fluid phases do not interact with each other. The total head is the sum of the gas and liquid head, adjusted according to the gas mass fraction. The total fluid approach includes fluid and thermodynamic properties of all components. Special care should be taken when the fluid contains water and/or MEG, as several of the normal utilised equation of state may not give reliable property data.

The total head for the total fluid model, Equation 2.10, is similar to the Schultz approach. The different is that properties takes account for multiphase flow and are therefore denoted MP.

$$H_{mp} = h_{2,\mathrm{mp}} - h_{1,\mathrm{mp}} = f_{s,\mathrm{mp}} \frac{n_{v,\mathrm{mp}}}{n_{v,\mathrm{mp}} - 1} \frac{\left(p_2 v_{2,\mathrm{mp}} - p_1 v_{1,\mathrm{mp}}\right)}{\eta_{p,\mathrm{mp}}} \tag{2.10}$$

Where

$$n_{v,mp} = \frac{\ln\left(\frac{p_2}{p_1}\right)}{\ln\left(\frac{v_{1,\mathrm{mp}}}{v_{2,mp}}\right)} \tag{2.11}$$

One of the major challenges with wet gas compression is lack of thermal equilibrium at the compressor outlet, documented by Hundseid [8]. The gas temperature increases substantially more than the liquid temperature, due to different heat capacities. The increased liquid content results in decreased outlet temperature, which greatly affect the isentropic efficiency. A real natural gas and condensate composition at 30 bar is examined in Figure 2.5, it displays how the discharge temperature affects the isentropic efficiency. An accurate wet gas compression analysis is important, but challenging due to the lack of thermal equilibrium.

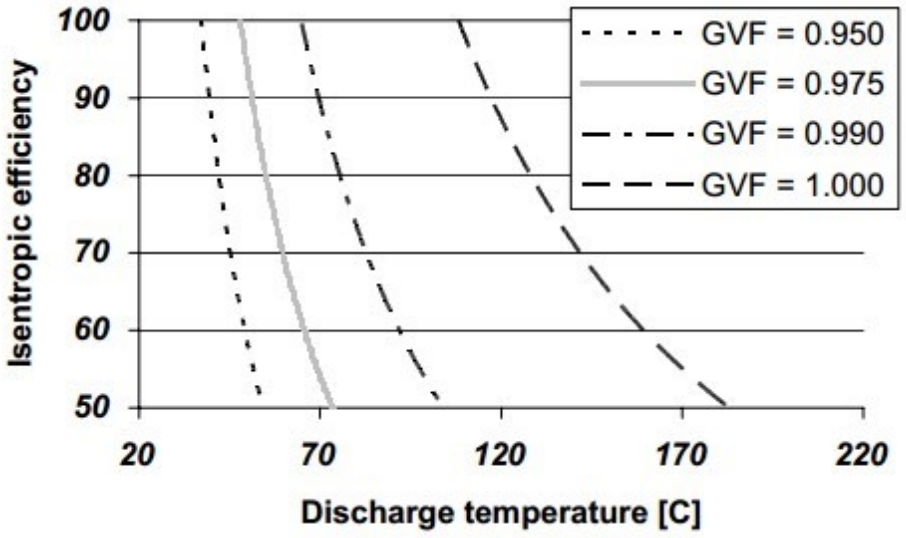

Figure 2.5: The impact of GVF on the isentropic efficiency [8].

2.3 Wet gas

This chapter will present the basics of wet gas theory. In order to understand the fundamentals of multiphase flow, expressions and relations will be introduced. The terminology presented will be used throughout the report.

Wet gas is defined as a multiphase flow where between 95% and 100% of the mixture consist of gas on volume basis and the remaining content is liquid [5]. An essential term when addressing wet gas is the Gas Volume Fraction (GVF), which is defined as:

$$GVF = \alpha = \frac{\dot{Q}_g}{\dot{Q}_{tot}} = \frac{\dot{Q}_g}{\dot{Q}_g + \dot{Q}_l} \tag{2.12}$$

Where $\dot{Q}_l$ and $\dot{Q}_g$ are representing the volume flow of liquid and gas, respectively. This relation also exists on the basis of mass. The Gas Mass Fraction (GMF) is defined as followed, where $\dot{m}_l$ and $\dot{m}_g$ represents the mass flow of the two phases:

$$GMF = \beta = \frac{\dot{m}_g}{\dot{m}_{tot}} = \frac{\dot{m}_g}{\dot{m}_g + \dot{m}_l} \tag{2.13}$$

The homogenous mixture of the multiphase wet gas can be calculated by Equation 2.14.

$$\rho_{mp} = \alpha\rho_g + (1 - \alpha)\rho_l \tag{2.14}$$

Equation 2.12 and 2.13 can be combined using the definition, $\dot{m} = \dot{Q}\rho$, to give a direct relation between GVF and GMF:

$$\text{GMF} = \frac{\alpha\rho_g}{\alpha\rho_g + (1 - \alpha)\rho_l} \tag{2.15}$$

The GMF and GVF are dominant parameters affecting the compressor performance. The GMF is directly associated with pressure increase and power consumption, whereas the GVF dominate the flow characteristic according to Grüner et al [9].

Maps categorizing the flow regime can be constructed depending on flow rates, geometry, fluid properties and are often based on superficial velocity. Superficial is referred to as the theoretical speed of a certain phase, assuming it occupies the entire cross-sectional area. Since wet gas is dominated by the gas phase (GVF>95%), it follows that superficial velocity for gas is considerably larger than for liquid. It is therefore expected that the wet gas flow regime is annular. Annular flow is characterised by a fast moving gas phase surrounded by a slow moving liquid film on the walls. Some liquids are present in the gas phase as droplets. The liquid film affect the flow through frictional forces and is larger at the bottom of the pipe due to gravity.

Slug flow is an important multiphase flow regime because it represents a potential danger for the compressor. Slug is characterized by large liquid sections that covers most of the pipe cross sectional area, separating the gas. For a wet gas compressor slugs represents variation in liquid content that affects the compressor performance.

2.4 Dimensionless parameters

This section will present important dimensionless parameters. An indication of fundamental flow behaviour can be obtained using non-dimensional parameters.

The density ratio is an important parameter in wet gas performance analysis as it reflects the of fluid homogeneity and the slip between phases. It is defined as:

$$\delta = \frac{\rho_g}{\rho_l} \tag{2.16}$$

The interface between the liquid and the dispersed phase is reflected by the viscosity ratio, see Equation 2.17. It also affects the velocity profile for the liquid and gaseous phase.

$$\gamma = \frac{\mu_g}{\mu_l} \tag{2.17}$$

The Stokes number characterize the droplets behaviour suspended in a fluid flow due to drag, see Equation 2.18. The number relates to the droplets and fluid response time as it's defined as the ratio of the characteristic time of a droplet to a characteristic time of the flow. At low Stokes numbers (St<<1), the droplets will follow the fluid streamlines completely. When the Stokes number is high (St>>1), there will be a large deviation between the droplet and fluid velocity resulting in different flow paths. For VIGV in wet gas condition this parameter is a particularly important because indicates whether the droplets follow the gas stream or not. If not, the VIGV performance reduces.

$$St = \frac{\tau C_{fluid}}{D_0} = \frac{Droplet\ response\ time}{Fluid\ respone\ time} \tag{2.18}$$

Where

$$\tau = \frac{\rho_d D_d^2}{18\mu_g} \tag{2.19}$$

The Mach number characterise the fluid relative compressibility. High compressor Mach number is associated with compressibility effects and shock waves, which greatly affects the compressor performance. In general, the identity of the fluid speed of sound and the critical velocity is not valid for a multiphase flow. Sonic speed may not coincide with critical speed, i.e. choking may occur and may not occur even though the Mach number is one.

$$Ma = \frac{c}{\sqrt{\frac{E}{\rho}}} = \frac{c}{\sqrt{\frac{dp}{d\rho}}} = \frac{c}{a} = \frac{Pressure\ forces}{Inertia\ forces} \tag{2.20}$$

The Mach number will change with the density ratio. Several speed of sound models exist, Wood's model is given by the Equation 2.21. This model is a simplification and assumes homogenous flow, local GVF variation in the flow and droplet size are not taken into account.

$$a_{mp} = \sqrt{a_g^2 \frac{1 + \frac{1-\alpha}{\alpha}}{\alpha\left(1 + \frac{1-\alpha}{\alpha}\frac{\rho_l}{\rho_g}\right)}} \tag{2.21}$$

The Weber number relates to the fact that interphase surface forces dominate the two phase fluid flow motion. It documents the fluid inertia compared to its surface tension, expressing droplet or bubble formation.

$$We = \frac{\rho c^2 D_d}{\sigma} = \frac{Inertia\ forces}{Surface\ tension\ forces} \tag{2.22}$$

Typical flow pattern can be described by Weber number. Weber number higher than 20 indicates that the inertia of the fluid defines the flow pattern, this typically relates to annular flow. At Weber number below 1, the surface tension is the dominate force, flow pattern will typically be bubbly, slug or droplet flow. Weber number between 1 and 20 are characterizes as a mixture of annular and droplet, bubble or slug flow. A droplet accelerated to a higher Weber number will gradually flatten until it reaches a critical Weber number where the surface tension is not strong enough to hold the droplet together. The droplet will break apart and form smaller droplets according to Rezkallah et al [10].

The Reynolds number relates to the ratio of inertial forces to viscous forces, specifying laminar or turbulent flow regime, including frictional flow loss coefficients, see Equation 2.23. It gives an indication whether the flow is dominated by turbulent of laminar flow, it also has a considerable influence on the flow frictional forces.

$$Re = \frac{Cd}{v} = \frac{\rho CD}{\mu} = \frac{Inertia\ forces}{Viscous\ forces} \tag{2.23}$$

However, calculating an accurate Reynolds number for multiphase flow is complex. It involves the calculation of stratified flow models with finite depth in combination with disperse flow models where the momentum exchange between the gas end liquid phases needs to be taken into account.

2.5 Compressor characteristics

This section will present dry and wet gas compressor performances. The VIGV affections on performance will be discussed in Chapter 3. A typical compressor map for dry gas is given and it is presented how wet gas affects the compressor performance. Challenges with wet gas compression will be discussed.

2.5.1 Dry gas performance

A typical compressor map for a centrifugal compressor is shown in Figure 2.6. The compressor operates between the surge line and the choke line. The surge line represents the limit of where instabilities occur, in this area stall and in the worst case backflow may occur which is a potential danger to the machine. Normally there is a control line which represents a safety margin to make sure the compressor stay out of surge. The choke line represents the limit of where subsonic conditions occur. At choke the lines of constant rotational speed becomes vertical, which implies that further decrease in head does not provide increased volume flow. The dashed elliptical lines represent compressor efficiency lines, with increasing efficiency to the middle. The compressor components are selected in order to give the design point a safe margin from surge and choke, and it lies at optimum efficiency.

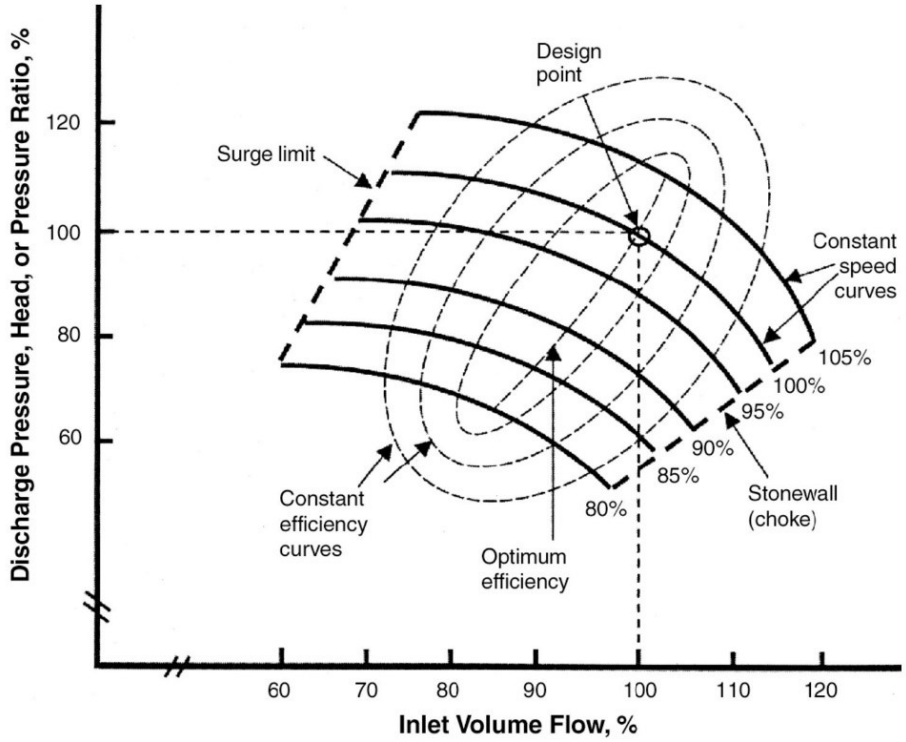

Figure 2.6: Typical centrifugal compressor map [11].

2.5.2 Wet gas performance

The presence of liquid phase changes the overall behaviour of the flow and thereby impacts the compressor performance. Multiphase flow is complex due to momentum, heat and mass transfer between the two phases, and this has influence on both the impeller and diffuser performance. In comparison to dry gas, the wet gas introduces compression losses that are not yet fully understood. Some of the important multiphase effects are non-thermal equilibrium, formation of liquid film and the influence of speed of sound. At present there exist no standards for performance evaluation of a wet gas compressor, due to the complexity of the multiphase flow making it difficult to develop precise correction methods [5].

Although it is difficult to calculate the wet gas performance, testing of wet gas compressors have been conducted, which provides an understanding of how wet gas influences the compressor performance. In 2004 Statoil tested a single stage centrifugal compressor designed for dry gas over a wide range of operational conditions and with a liquid content up to 3% on a volume basis [12]. The results of these tests are shown in Figures 2.7, 2.8 and 2.9.

Figure 2.7 shows that the polytropic head decreases significantly when increasing the liquid content. In addition, the figure shows that the inlet pressure or density is an important factor in wet gas performance. The density ratio is dependent on the suction pressure, as well as content and composition of the liquid and gas used.

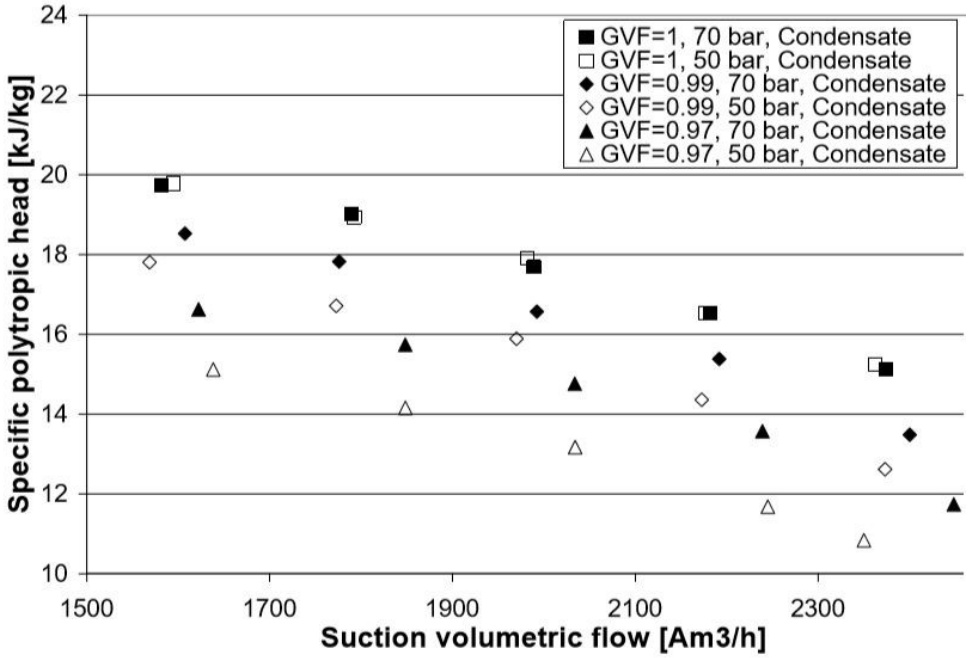

Figure 2.7: Polytrophic head for wet gas [12].

Figure 2.8 is presenting typical changes in pressure ratio between dry and wet gas. Here it is shown that pressure ratio is increasing with higher liquid content.

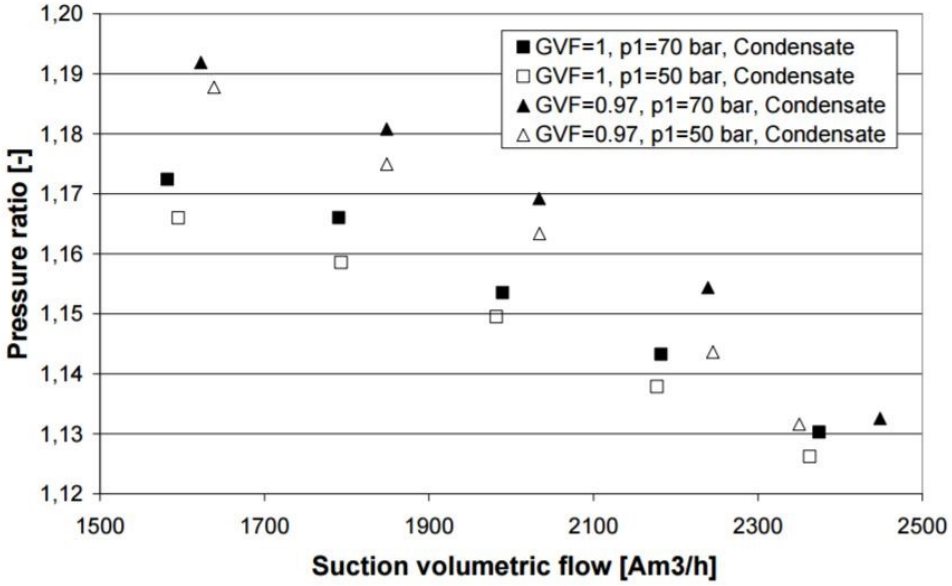

Figure 2.8: Pressure ratio for wet gas [12].

The presence of liquid changes the internal losses through both friction and compressibility effects. In Figure 2.9, a considerable reduction in polytropic efficiency is observed when increasing the liquid content. In addition, reducing the inlet pressure has a negative effect on the efficiency.

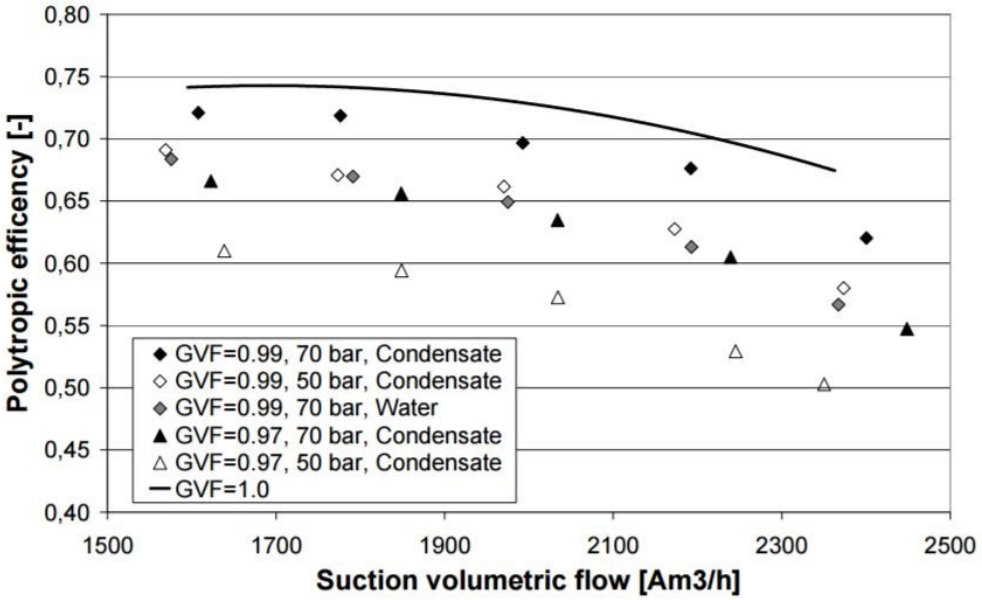

Figure 2.9: Polytropic efficiency for wet gas [12].

Bertoneri et al [13] tested a single stage centrifugal compressor in a closed loop with an air and water mixture. In Figure 2.10 the pressure ratio is plotted against the volume flow coefficient for several wet gas cases. Increased liquid content gives higher pressure ratio at low volume flow, at high volume flow the pressure ratio is decreasing with increasing liquid content. The increase pressure ratio is explained by higher density, the cooling effect of water and the speed of sound variation in a two phase environment.

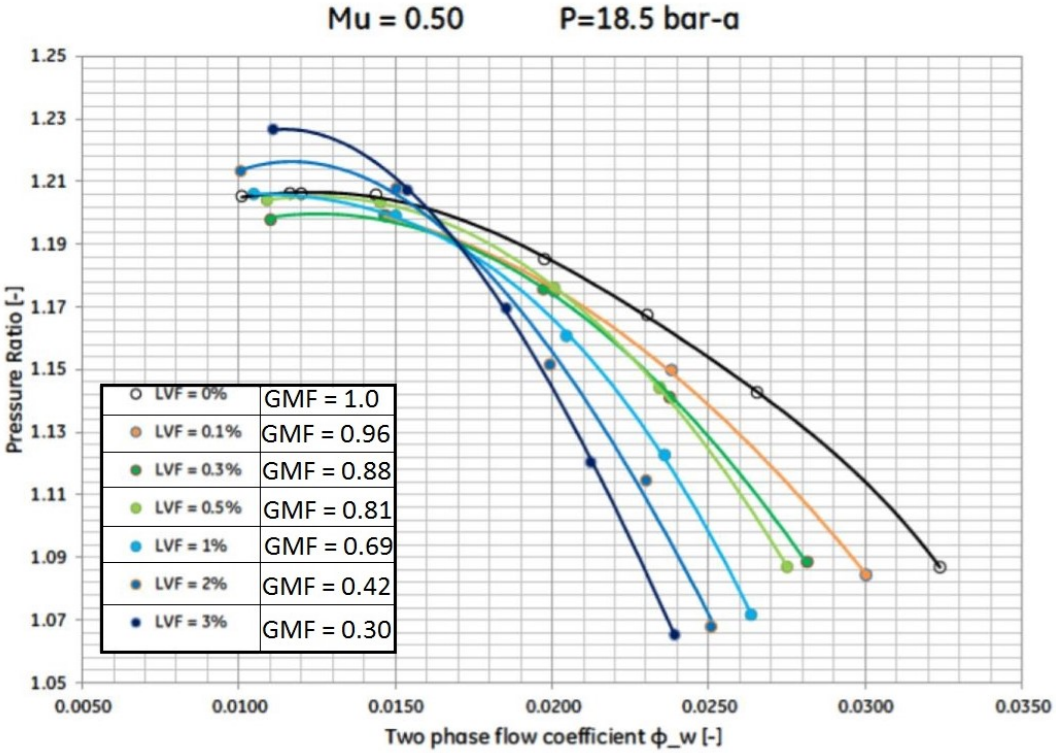

Figure 2.10: Pressure ratio over the compressor with several different GMFs [13].

The reduced performance at high volume flow is due to increased blockage in the diffuser. This reduced diffuser performance can be seen by looking at Figure 2.11. Here, the pressure ratio over the impeller is plotted against the volume flow coefficient. The increased liquid content results in increased pressure ratio almost independent of volume flow. Bertoneri explains that the poor behaviour of the diffusor is due to unconventional design (two parts were used), flow angle change, water-wall splashing and increased overall frictional forces.

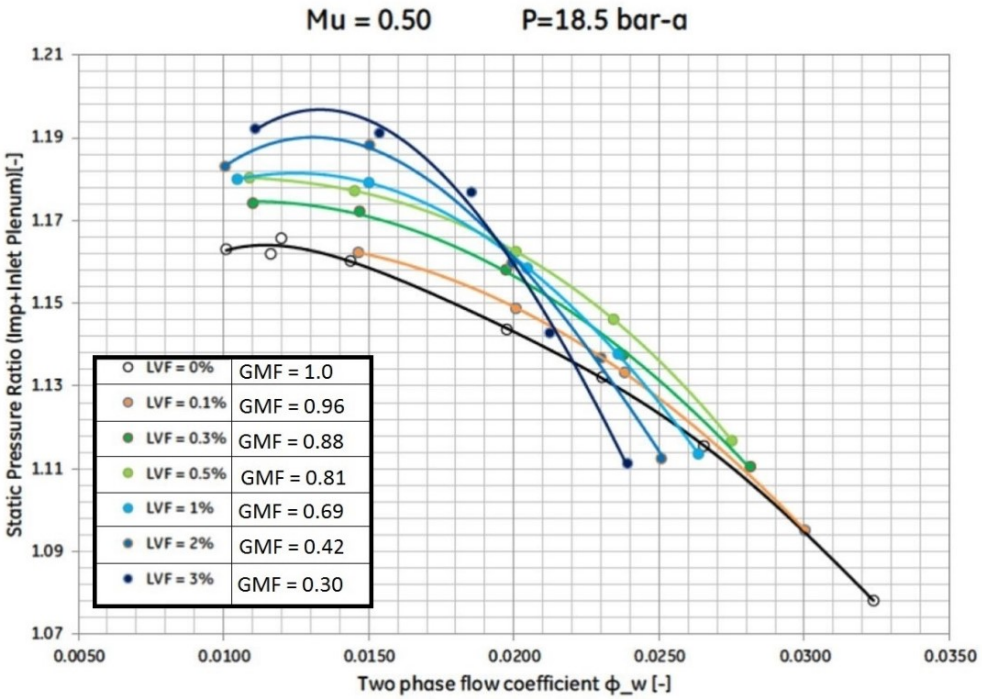

Figure 2.11: Pressure ratio over the impeller with several GMFs [13].

Ferrara [14] has tested a single stage centrifugal compressor with an air and water mixture at the NTNU test facility, the same compressor as presented in Chapter 4. Figure 2.12 shows her results as the function of pressure ratio versus volume flow. In comparison with Bertoneri, the lines for wet gas are not as steep. For GMF 0.95 the water presence does not significantly affect the pressure ratio with respect to dry conditions.

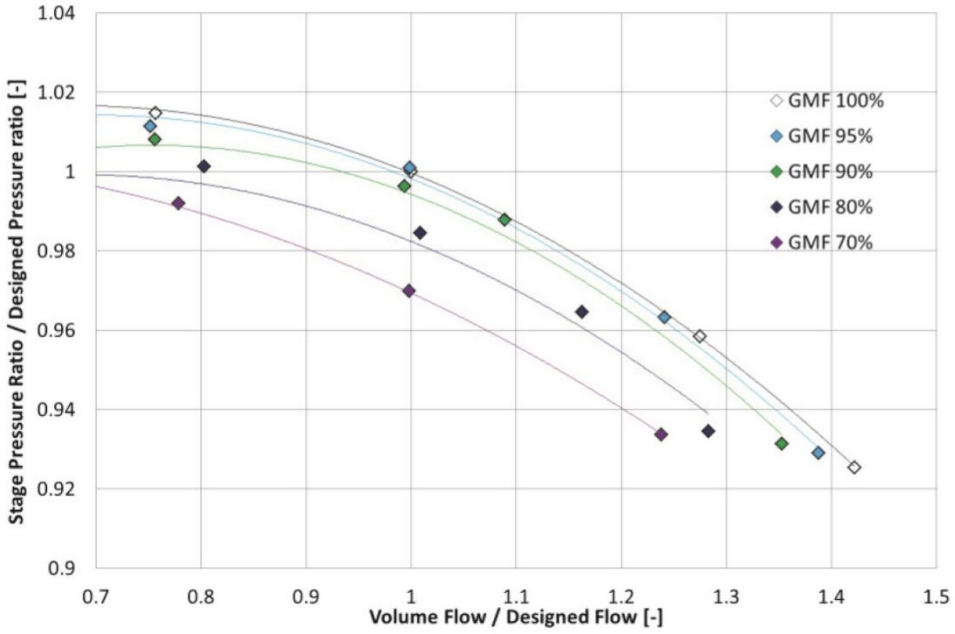

Figure 2.12: Pressure ratio for wet gas, from the NTNU test facility [14].

To conclude, a small liquid fraction down to GMF 0.98-0.97 seems to increase the pressure ratio. With a GMF at 0.95 the performance lies close to the dry cases, but when the liquid content increase further the performance drops. This can be explained by the fact that liquids increase the pressure ratio, but when the fraction of liquid becomes high enough, the compression losses induced by the liquid counteracts the positive effect. However, the greatest pressure ratio is achieved at low GMF (0.4-0.3), but at these liquid fractions the operating range is small, represented by steep curves. Note that the compression losses increase at high volume flow, this could imply that the liquid leads to blockage in the diffusor and this effect is enhanced at high volume flow.

3. Variable inlet guide vanes

The IGV are stationary blades mounted on the compressor casing, upstream of the impeller. The guide vanes enable control of the impeller inlet angle and changing that directly affects the compressor characteristics and stability. The compressor can be operated at its best operational point, even at off-design conditions by changing the angle of the VIGV.

IGV may be added to an existing system to handle with inefficiency at the impeller eye, by improving the guiding and distribution of the flow. Industrial compressors with varying operational conditions are often fitted with VIGV to improve off design performance. Guide vanes can also be found in several gas turbine and turbocharger applications. A VIGV assembly for fan is depicted in Figure 3.1, the vanes are turned by rotating actuator ring on the outer casing.

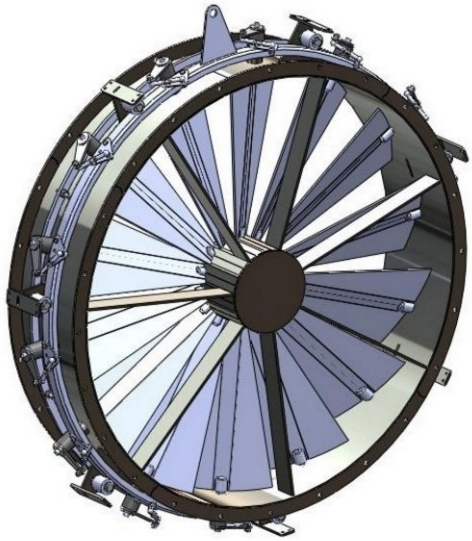

Figure 3.1: Inlet guide vane assemble for a fan [15].

This chapter aims to present the principle of operation, dry gas performance and wet gas performance. In addition, compressibility effects and stability consideration will be evaluated. The VIGV will only be discussed in conjunction with centrifugal compressor.

3.1 Principle of operation

This section will present the principle of operation for the IGV and show how it interacts with the impeller.

3.1.1 The inlet guide vane

The nomenclature on a cascade for airfoil is presented in Figure 3.2, and will be used throughout the report.

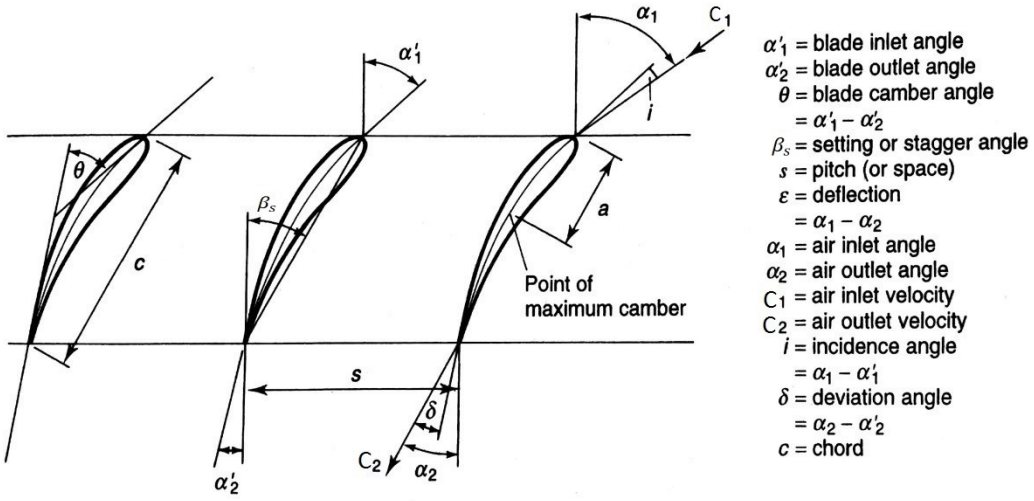

Figure 3.2: Blade nomenclature [4].

The impact of a single guide vane on a flow field can be seen in Figure 3.3. C_o is the velocity approaching the IGV, while C_1 is the velocity out of the IGV and into the impeller. On the right hand side, the velocity triangle out of the IGV is shown. C_1 is decomposed into an axial component C_{a1}, and a tangential component C_{w1}.

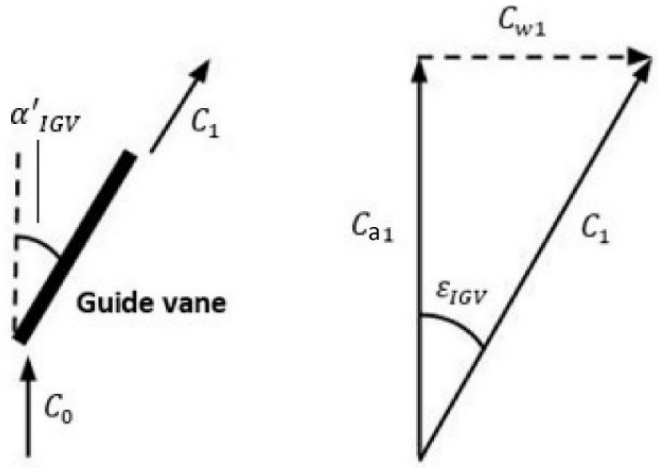

Figure 3.3: Inlet guide vane in axial flow.

An increase in blade angle will lead to increased prewhirl. The nomenclature in Figure 3.4 is analogous to Figure 3.3, the notation is slightly different in order to differ from IGV and impeller angles. An axial inlet velocity is assumed both for this section and the following. This implies that $i_{IGV} = \alpha'_{IGV}$. For low incidence angles $\alpha'_{IGV} = \varepsilon_{IGV}$, can be assumed. As the guide vanes keep turning, the blade angle and the turning angle tends to deviate increasingly up to a point where separation occur. Separation influences the compressor performance.

In Figure 3.4, the interaction between the guide vane and impeller can be seen. The inlet velocity triangle and the impeller incidence angle i_{Imp}, are directly affected by the prewhirl provided by the IGV. β_1 represents the angle between the relative velocity and the axial velocity.

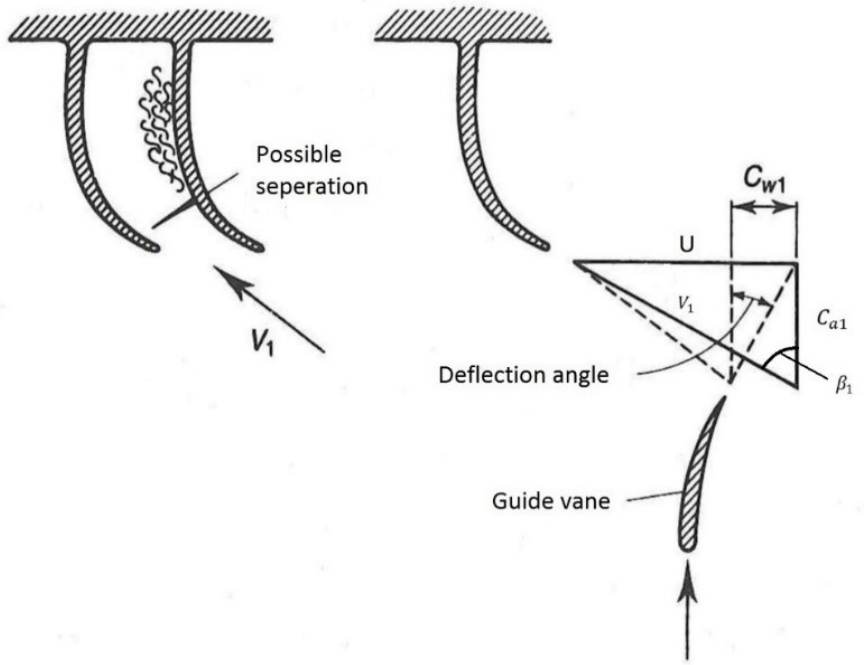

Figure 3.4: Interaction between IGV and impeller [4].

The maximum capacity of the impeller can be found when the cross sectional area is greatest. This happens when $i_{Imp} = 0°$. Frictional and compressibility losses are reduced by improving the incidence angle towards the impeller [4]. The optimal i_{Imp} can be achieved by changing the prewhirl provided by the IGV. How β_1 scales with prewhirl provided is shown here:

$$\beta_1 = tan^{-1}\left(\frac{U - C_{w1}}{C_{a1}}\right) \tag{3.1}$$

Separation could occur on the impeller suction side if β_1, and thereby i_{Imp}, is increased sufficiently. This will affect the compressor performance.

3.1.2 Inlet guide vane performance

The aerodynamic behaviour of a VIGV has been investigated by Händel and Niehus [16]. Their experiment was conducted on a 2D linear cascade with straight symmetric blades. Figure 3.5 Shows the Mach number distribution over the axial chord at different stagger angles, β_s. The stagger angle is defined in Figure 3.2. A stagger angle of 90° gives an incident IGV angle of 0°, and a β_s equal to 80° gives a i_{IGV} equal to 10°, and so on. The Mach number is presented for both the pressure and the suction side, when β_s equal 90 ° no change in Mach number is experienced due to symmetry.

The Mach number is greatly affected by the stagger angle. Maximum Mach number for β_s equal to 70° is almost twice as large it is at the trailing edge. β_s equal to 90° only gives a 30% increase. A change in stagger angle has proven to increase the Mach number at the suction side. Although, when β_s is equal to 60°, the Mach number at the suction side drops. This is because the flow separates close to the leading edge without reattaching, this leads to acceleration of the flow along the entire pressure side.

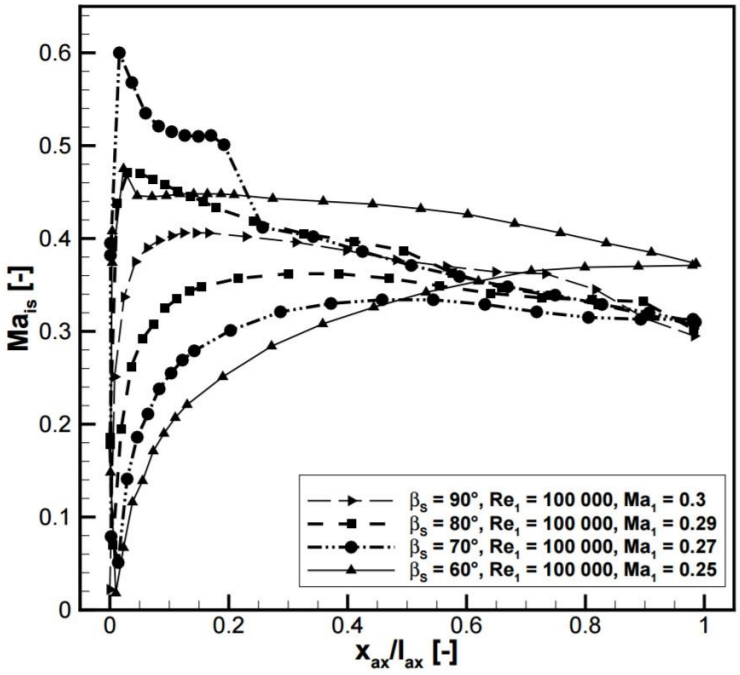

Figure 3.5: Mach number distribution for different stagger angles [16].

The separation leads to significant increase in pressure loss, this can be seen in Figure 3.6 where the total pressure loss is plotted against Reynolds number for different stagger angles. Increased incident angles, analogous to decreased stagger angles, lead to higher pressure losses. The biggest occur at β_s equal to 60° because of the flow separation. In addition, the pressure losses increase with decreasing Reynolds numbers.

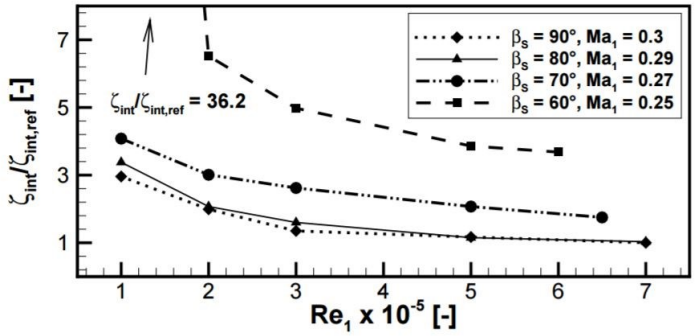

Figure 3.6: Pressure losses for various Reynolds number and stagger angles [16].

The optimal impeller incidence angle can be obtained by adjusting the prewhirl provided by the IGV. However, matching the optimal incidence angle over the entire blade is challenging. This is due to the fact that the velocity triangle changes from hub to tip as the impeller velocity is a function of the radius. The guide vanes are normally twisted to accommodate for this, by giving them a three dimensional design. The prewhirl is increased from hub to tip to be able to meet the best operational point.

3.2 Cascade theory and secondary losses

When evaluating the aerodynamic performance of compressors and turbines is it important to have an understanding of the cascade theory. An introduction to cascade theory and a presentation of secondary losses will be given in this section.

Cascade test are commonly used when evaluating flow effects for compressor and turbine experiment. A cascade consists of a fixed duct with stationary blades where air is supplied upstream. Circular configurations can be used, although it is more common with two-dimensional geometry. To determine the aerodynamic effects on the blades are the overall goal of the cascade. When it comes to compressors and turbines, the desired result is to minimize the drag and maximise the lift. Other parameters of interest are deflection angles, secondary losses, separation and instability.

The IGV system is essentially a circular cascade. Thus, experimental results obtained by cascade testing can be used to predict the performance of an IGV system.

Secondary losses are of vital importance when evaluating rotating equipment and cascades. One form of the secondary losses is tip clearance. Tip clearance is associated with stagnation pressure loss and reduced flow turning. For an IGV assembly, these effects will affect the compressor performance downstream. Hence, tip clearance should be as small as possible.

Another form of secondary losses is trailing tip losses. The stagnation pressure loss occurring on the trailing edge of the blades in a cascade is presented in Figure 3.7.

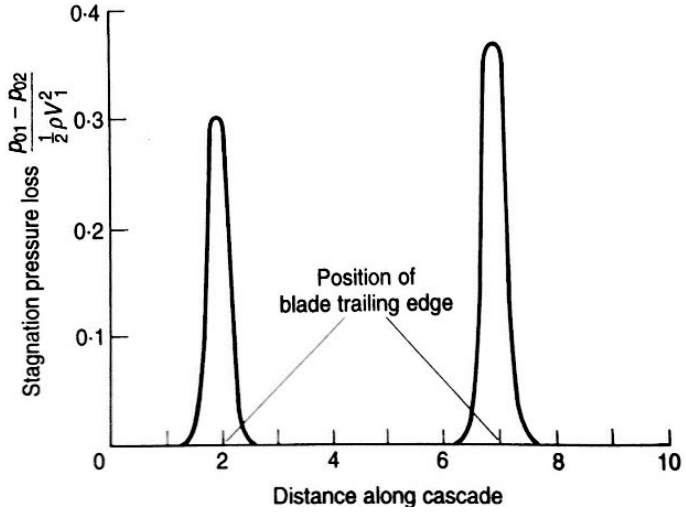

Figure 3.7: Stagnation pressure loss along cascade [34.

Endwall flow are an important source of secondary losses. A phenomenon called horse-shoe vortex was described by Lampert [17] as he investigated endwall flows. It forms on the suction side of the blade and is presented in Figure 3.8.

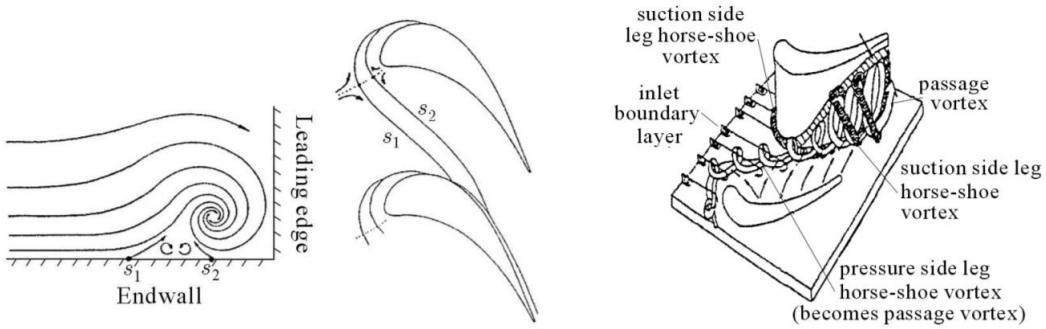

(a) Formation of the horse-shoe vortex *(b) Propagation of the horse-shoe vortex*

Figure 3.8: The horse-shoe vortex [17].

The boundary layer stagnates slightly upstream of the leading edge, forming to saddle points, s_1 and s_2. Before being transported downstream in two legs, the boundary layer is rolled up in a recirculating zone. The two legs are named pressure and suction side of the horse-shoe vortex. The pressure leg moves across the passage to the nearby suction side of another blade. This results in a vortex propagation in radial direction along the suction side of the blade.

3.3 Dry gas performance

The variable IGV will affect the flow field, compressor head and stability. This section will present the IGV impact on compressor performance and operational characteristics. Emphasis will be put on compressibility effect, stability and compressor characteristics.

3.3.1 Compressibility effect and stability consideration

Mach numbers must be evaluated for the highest velocities. In centrifugal compressors, the greatest velocity is the relative velocity at the inlet of the impeller. The relative Mach number is therefore:

$$Ma_{rel} = \frac{V_1}{\sqrt{\kappa RT}} \tag{3.2}$$

When M > 1 shockwaves form, resulting in great pressure losses and poor compressor performance. On the other hand, it is desirable to have as high velocity as possible to maximise the volume flow. With IGV it is possible to change the relative velocity, this can be seen in Figure 3.9. The dotted lines represent the velocity triangle after an IGV has induced a prewhirl, upstream the impeller. The IGV can also provide a counter whirl in the opposite direction that will give an increased relative velocity and improved compressor performance, provided that no enhanced losses occur.

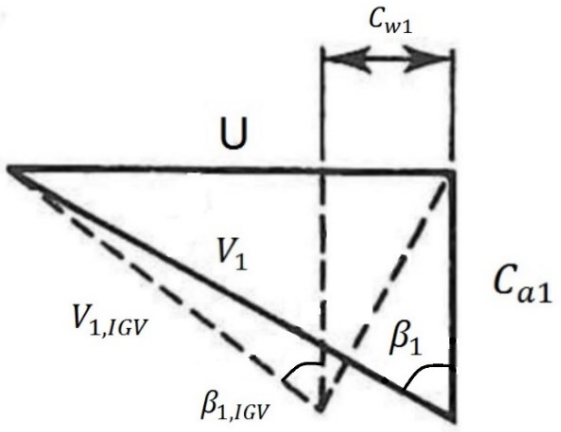

Figure 3.9: IGV effects on the relative velocity.

The relative velocity can be calculated by equation (6.3) and (6.4), where the latter yields in the case on an imposed prewhirl.

$$V_1 = \sqrt{U^2 + C_{a1}^2} \tag{3.3}$$

$$V_{1,IGV} = \sqrt{(U - C_{w1})^2 + C_{a1}^2} \tag{3.4}$$

High Mach numbers are associated with increased compressibility losses which are sensitive to the incidence angle [4]. Figure 3.10 shows the compressibility losses for an axial compressor at different Mach numbers and incidence angles.

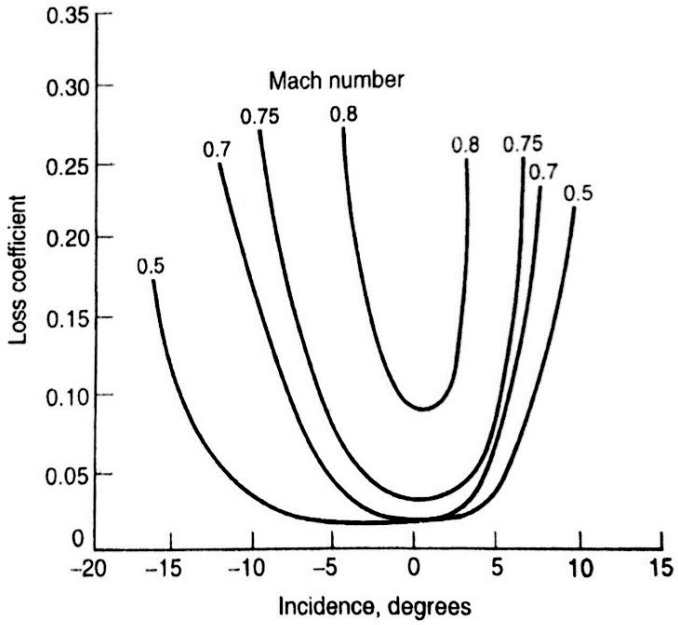

Figure 3.10: Losses influenced by Mach number and incidence angle [4].

With a variable inlet guide system, a compressor can maintain high volume flow while avoiding shock formation by an efficient control of V_1. In addition to reduce the performance and increase the mechanical wear, shock formation tends to have impact on the stability by affecting the upstream velocity profile.

Blade stalling is highly undesirable and induces compressor instabilities. This occurs when the impeller incidence angle is increasing enough to make the flow detach from the suction side of the impeller vane. The stalling of one blade, will affect the nearby blades and develop into stalling at all blades. A compressor driven at higher speed generally goes directly from stable operation to separation at all blades. This will reduce flow throughput and pressure generated over the compressor. Stall is often followed by surge, causing backflow. Surge is associated with instabilities, poor compressor performance and potential mechanical damage. Stall is a well-known aerodynamic phenomenon, Figure 3.11 shows how stall can occur over an airfoil.

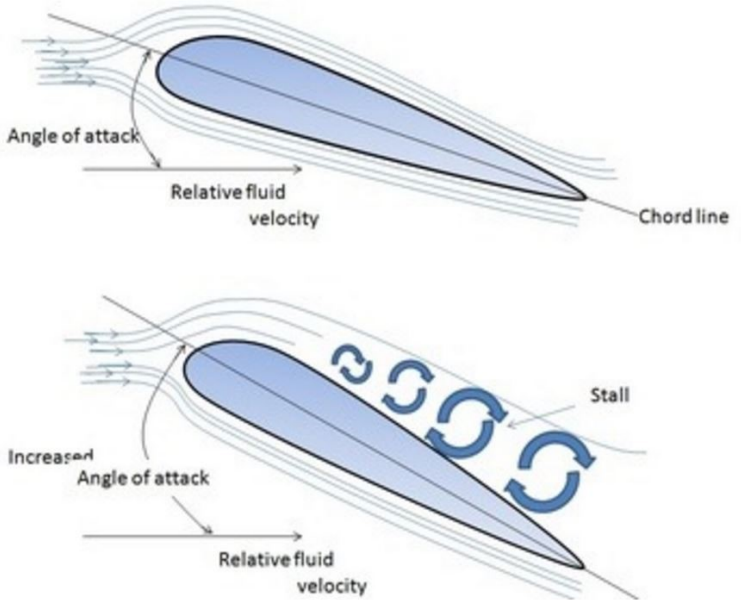

Figure 3.11: Stall over an airfoil [18].

To ensure stabile compressor operations it is important to prevent stalling. This is possible by utilizing IGV system to induce a prewhirl upstream the impeller that reduces i_{Imp}. If instabilities have already occurred, it is possible to use an IGV system to move out of the surge area and stall ceases.

3.3.2 Compressor characteristics

The compressor performance map for variable speed and VIGV is shown in Figure 3.12. Note that the dotted lines only represent change in VIGV. The axes are expressed in ratios of relative to the nominal head and volume flow rate. The top line represents no prewhirl while the lower lines are at high prewhirl in the direction of the flow. The operational range for VIGV is well within the surge limited of variable speed only, this means that the compressor can move out of surge with using IGV and thereby maintain stable operation.

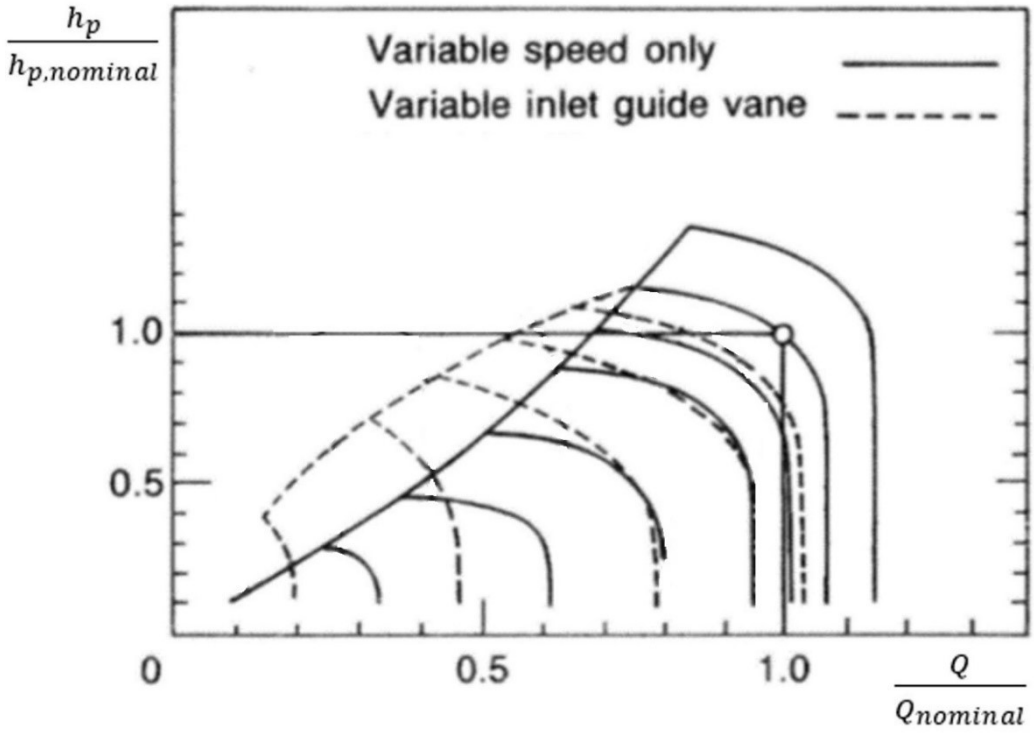

Figure 3.12: Compressor performance with VIGV [19].

The compressor chokes at lower pressure with IGV because it is essentially an obstacle for the flow. This explains why the dotted VIGV lines in the figure becomes vertical, which shows that the volume flow will not increase even though the head decrease. Swain and Coppinger [20] investigated pressure drop over a VIGV assembly, their results show a remarkable pressure drop at large blade angles. Noted that a VIGV assembly at full open position, will induce a pressure loss that should be taken into account.

The performance curves for a fixed speed centrifugal compressor with VIGV are shown in Figure 3.13. Where 100% indicates no prewhirl, values over 100% represents the counter-rotating prewhirl while lower values represent prewhirl in the same direction of the rotation. The best efficiency line marks a desired compressor operation point, and farther away from this line leads to decreased efficiency.

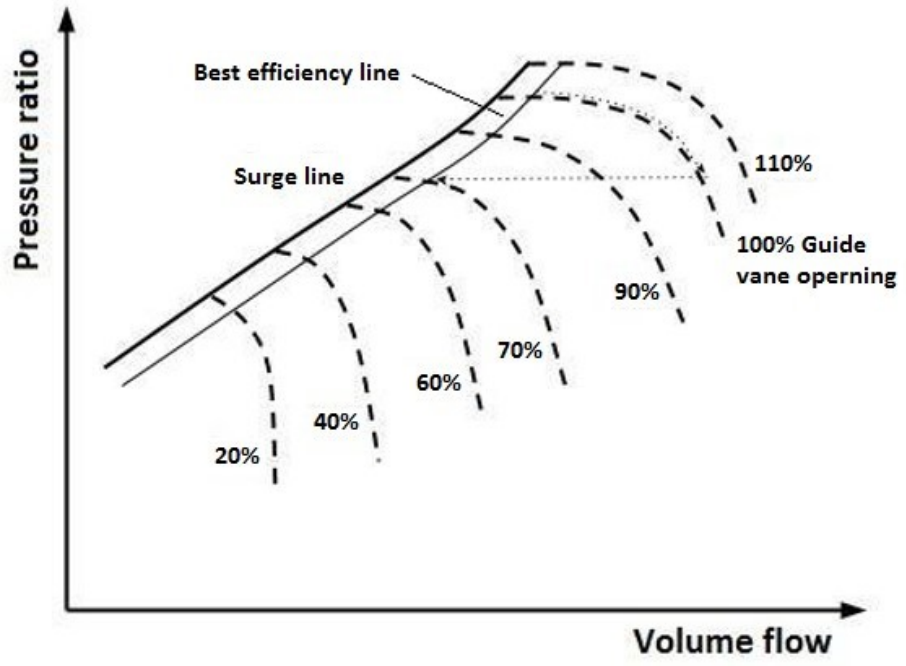

Figure 3.13: VIGV performance curves [21].

When a fixed speed compressor is forced to be operated at off-design conditions, the efficiency decreases. The IGV can be used to improve the efficiency, an example of this is shown in Figure 3.13. The compressor is operated at 100% IGV and the efficiency is poor, when reducing the IGV to 70% the pressure ratio remains the same and the compressor efficiency improves. However, the increased prewhirl reduces the volume flow rate.

In order to fully understand how changing the IGV angler affects the compressor performance, the relation between the velocities triangles and compressor performance needs to be known. Figure 3.14 shows how the inlet velocity triangle is affected by changing the IGV angle. Here represented by three different setting, (a) zero prewhirl, (b) prewhirl and (c) counter whirl.

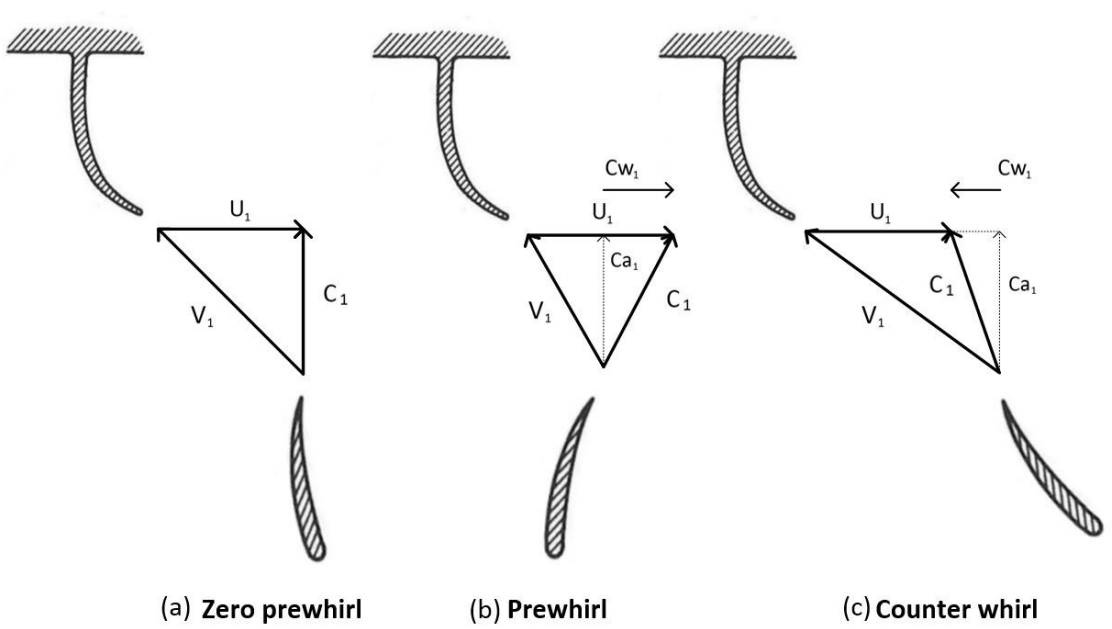

Figure 3.14: How the IGV affects the inlet velocity triangle.

How these different velocities triangles affects the compressor performance can be seen in the Euler head Equation 3.5. The impeller outlet velocities, denoted 2, are independent of the inlet angle. At zero prewhirl, the C_{w1} component equals zero as the C_1 is only in the axial direction and the head is solely dependent of the velocities out of the impeller. At prewhirl the head reduces as it gives a positive C_{w1} component. Counter whirl gives a C_{w1} in other direction, meaning it is a negative component and therefore the head increases.

$$h = (C_{w2}r_2 - C_{w1}r_1) \tag{3.5}$$

Figure 3.15 is a compressor map showing that the three different cases gives different compressor curves. The lines going from (b) to (a) and to (c) represent how the compressor will react when changing the compressor from prewhirl, through zero prewhirl, to counter whirl.

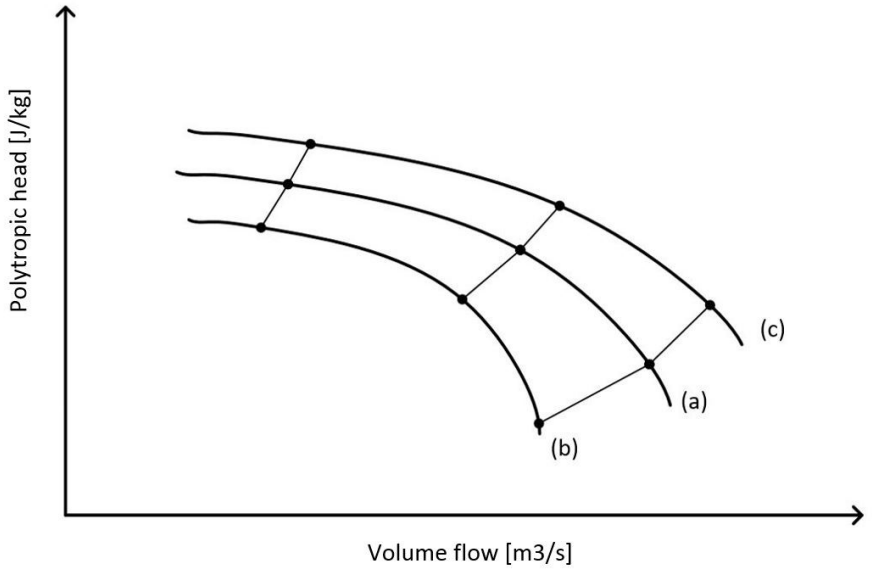

Figure 3.15: How changing the IGV angle affects the compressor performance.

Lüdtke [22] performed a case study to compare four different compressor regulation methods; variable speed, suction throttling, VIGV and bypassing. Variable speed was the most energy effective, followed by VIGV and suction throttling, bypassing is the least energy effective. An interesting founding was that the surge occurred at lowest volume flow with the VIGV. Even though centrifugal compressors have several stages, having a row of VIGV before the first stage effects the performance of the hole compressor, especially for high-Mach-number compressors [22].

3.4 Wet gas performance

This section will evaluate some of the effects and challenges experienced in wet gas compression. Discussions will be made on how the change from dry to wet gas influence the blade aerodynamics and the VIGV performance.

When changing from dry to wet gas, several effects are experienced. The fundamental properties of the mixture changes, including increased density. The behaviour of the flow is changed by the inertia of the droplets and the formation of liquid film on the walls and vanes. Due to non-equilibrium state of the mixture, a continuous interaction of heat, mass and momentum exchange are experienced [5].

It has been observed that the gas phase travels faster than the liquid phase, this leads to drag force between the two phases. The velocity profile upstream of the impeller differs remarkably in comparison to the dry gas scenario. In addition, the speed of sound reduces and the erosion effects are increased. All these effects have an impact on the wet gas compression performance.

3.4.1 Aerodynamic performance

Several experiments have been conducted regarding airfoils exposed to wet gas, and the IGV is essentially a cascade of fixed airfoils.

Grüner et. al. [23] investigated the aerodynamic effect of an airfoil in wet gas flow. The test included different incident angles and gas volume fractions. The results show a liquid film formation on the suction side of the airfoil. Increased film thickening was experienced at incidence angle higher than 0° and at reduced GVF. A large boundary layer separation can be seen in Figure 3.16.

Figure 3.16: GVF 0.990 and 0.970 at incidence angle of 0° [23].

A continuity wave was observed surrounding the airfoil, described as a boundary region of low GVF. This separates the incoming flow from the flow adjacent to the blade. The continuity wave is depicted in Figure 3.17, it has a clear U-shaped profile with high liquid content.

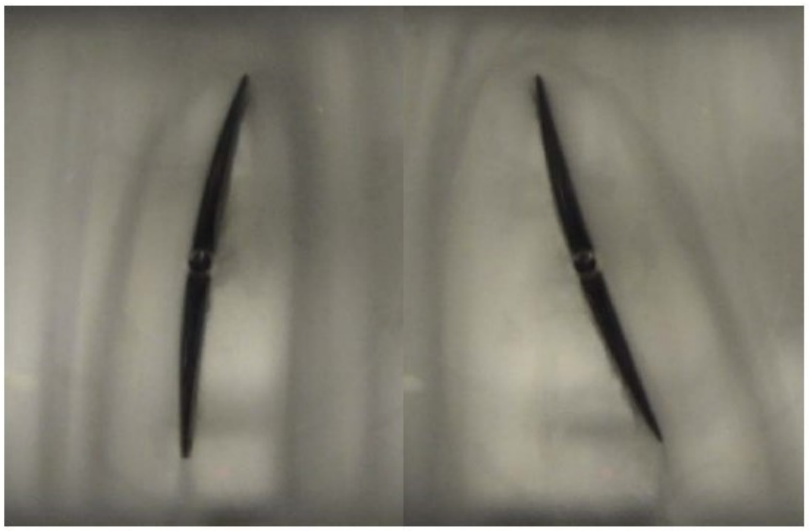

Figure 3.17: Continuity wave at GVF 0.99, incidence angle of -16° and 12° [23].

Grüner concluded that reduced GVF results in more liquid deposition, which increases the pressure drop. The premature boundary layer separation degrades the airfoil performance at higher liquid mass flow. Considerable limitations on the operational characteristic of the compressor are set by the separation. Grüner imposes that the continuity wave may cause changes to the flow angle into the impeller and diffuser, and change the local speed of sound due to high liquid concentrations. However, the effect of the continuity wave is somewhat unclear.

The influence of water droplets in a compressor cascade was investigated by Ulrich and Joos [24]. Water droplets was injected at lower velocities than the surrounding air entering the cascade. A Phase-Doppler-Anemometry was used to measure the velocity and the size of the water droplets. Their results indicate that the velocity field around the airfoil drops when water is injected, the velocity distributions are depicted in Figure 3.18.

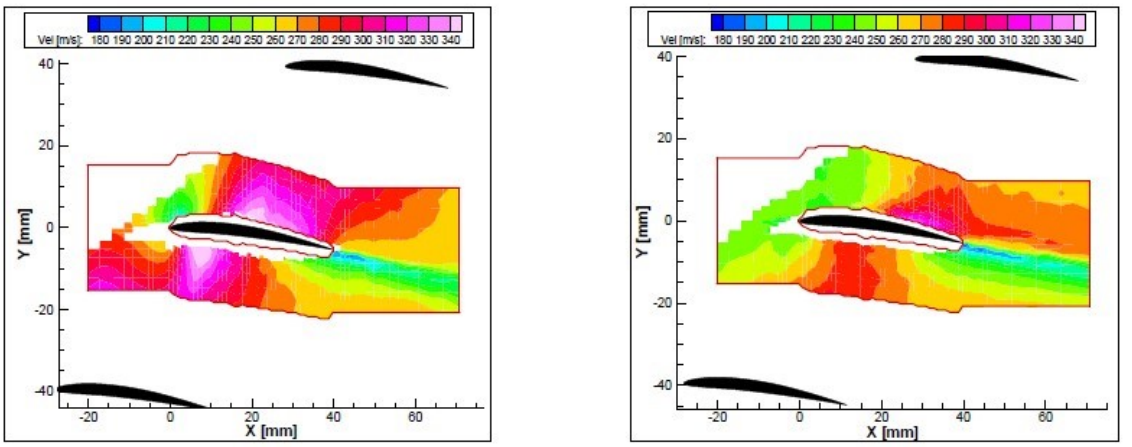

(a) Without water *(b) With water*

Figure 3.18: Velocity field over airfoil [24].

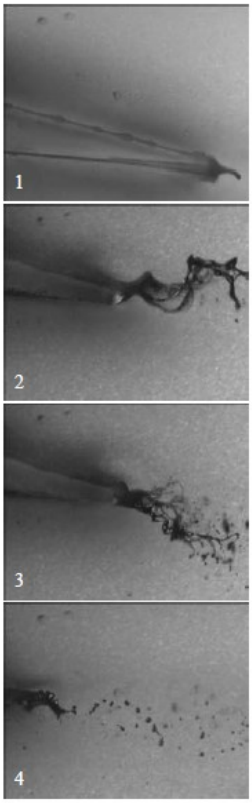

Figure 3.19: Liquid formation and droplet breakup [24].

Their experiment also evaluated the ligament formation and droplet breakup at the trailing edge. On the airfoil, droplets accumulate to form a shear driven film moving towards the trailing edge. The water builds up at the edge, forming a growing droplet (1). It grows until a certain size is achieved, and it forms into a ligament (2 & 3), as depicted in Figure 3.19. These ligaments are exposed to Rayleigh-Taylor instabilities, and eventually breaks up and form droplets (4).

Ulrich and Joos concluded that for water injected flows of gas turbines or industrial compressors, the flow field around the airfoils has to be taken into account. Furthermore, the velocity distribution may have an effect on the efficiency. Further emphasis were pointed towards droplet trajectories regarding erosion assessment.

3.4.2 Stability and erosion considerations

The instability characteristics on a single-stage centrifugal compressor exposed to both dry and wet gas was investigated by Grüner [25]. The results show that the surge margin is increased when the liquid content is increased. Figure 3.20 show the effects of different GMFs on the compressor characteristics.

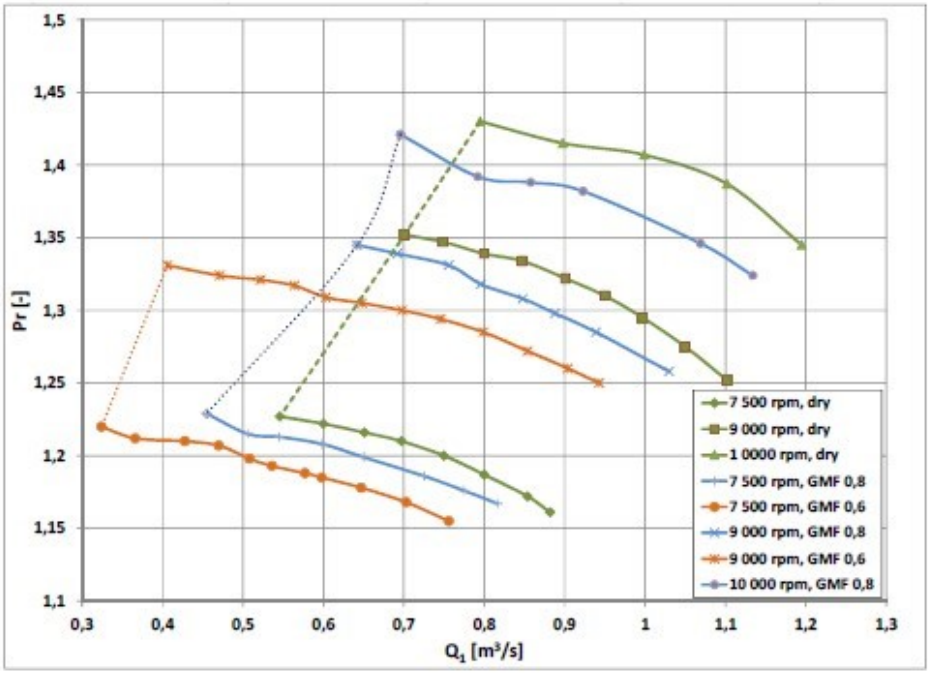

Figure 3.20: The surge lift at varying GMF [25].

With the basis of dry gas performance, it is expected that IGV will increase the positive impact on surge and stability for wet gas.

Erosion is a challenge in turbo machinery. Wet gas compressors are experiencing an enhanced erosion effect due to the presence of high density liquid droplets. The slip between the phases and the inertia of the droplets impose erosion challenges. Increased velocities enhance erosion effects, in that context IGV may reduce erosion by inducing a prewhirl which reduces the relative velocity. In addition, an optimal angle can be obtained by using IGV, reducing the erosion.

Liquid accumulation is a common problem in steam turbines. The water accumulate on the upstream stator vanes, the liquid film moves slowly towards the trailing edge where it breaks off and re-joins the flow. The droplets have a much lower velocity than the steam and tends to collide on the turbine suction side, where erosion normally occur. The same phenomenon can be expected when having a IGV in wet gas, although the erosion is expected to occur on the pressure side.

3.4.3 Compressor characteristic

Vigdal et al [26] have investigated how VIGV influence the compressor performance in wet gas flow. The impeller flow direction was varied between -20° counter whirl and 40 ° prewhirl. In addition, the inlet GMF was varied between 1.0 and 0.4. The test results found at the NTNU test facility are presented in Figure 3.21. The VIGVs introduces little to no pressure loss at GMF 1.0 and 0.8, compared to the scenario with no VIGVs installed. When increasing the liquid content however, it is evident that increased pressure loss introduced by the VIGV reduces the compressor pressure ratio. Additionally, the increased liquid content gives a reduction in the VIGV effect on pressure ratio and volume flow.

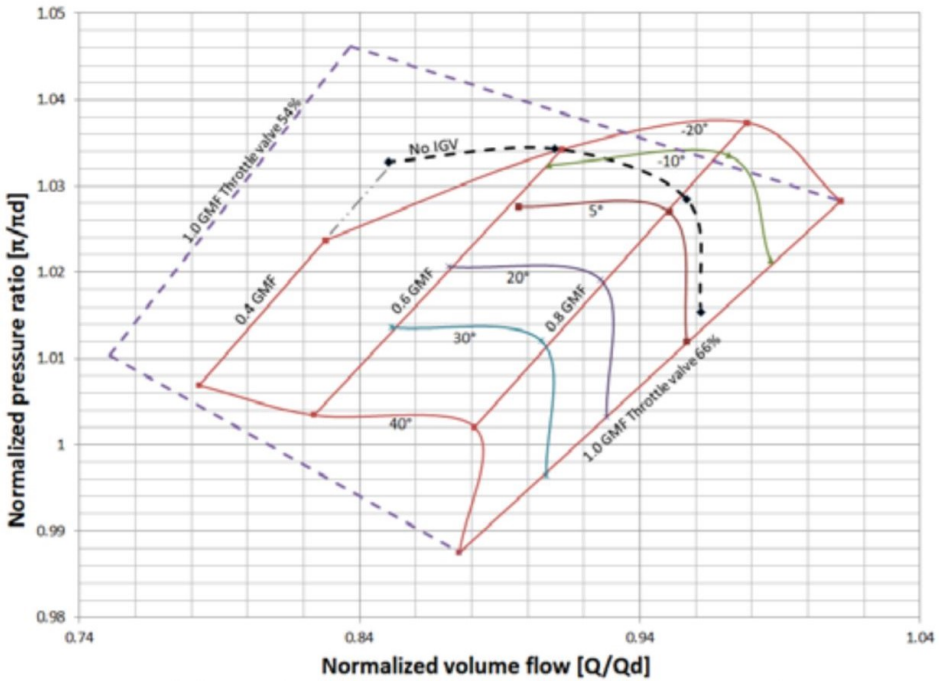

Figure 3.21: VIGV effect on the compressor map [26].

Vigdal concludes that the performance of VIGVs decreases with enhanced liquid content. At higher liquid content, the VIGV ability to guide the flow decreases due to increased momentum transfer between liquid and gaseous phase. The effect of VIGV per change of setting angle is greater at prewhirl than with counter whirl. This is because of the greater compression losses experienced with the VIGVs at wet gas flow. These losses will reduce the effect of counter whirl and increase the effect of prewhirl.

3.5 Summarized viable inlet guide vanes

The VIGV affect the compressor performance by inducing a prewhirl at the compressor inlet. Compressibility effects and compressor stability are influenced by the prewhirl provided. By utilization of VIGVs the compressor can operate at best efficiency point even at off-design conditions. When changing from dry to wet gas, several effects are experienced; a shift in stability, the aerodynamic performance changes and erosion increases. Droplet accumulation and continuity waves influence the flow field around the vanes. Increasing liquid content reduces the VIGV performance and the effect of VIGV is greater at prewhirl than with counter whirl.

4. NTNU test facility

This chapter will present the NTNU compressor test facility which were used to obtain the results in Chapter 6. Emphasis is put on the VIGV assembly, the compressor rig is well documented by Hundseid et al [27].

4.1 The compressor rig

The test facility was at the time of the experiments an open loop configuration where ambient air entered a stainless steel pipe, about 15 meters upstream of the impeller intake. The air flowed through an orifice meter, measuring the volume flow. Downstream the orifice meter an inlet valve followed, along with several temperature and pressure sensors before reaching the water injection system. A pipe and instrumentation diagram (P&ID) of the test rig is presented in Figure 4.1.

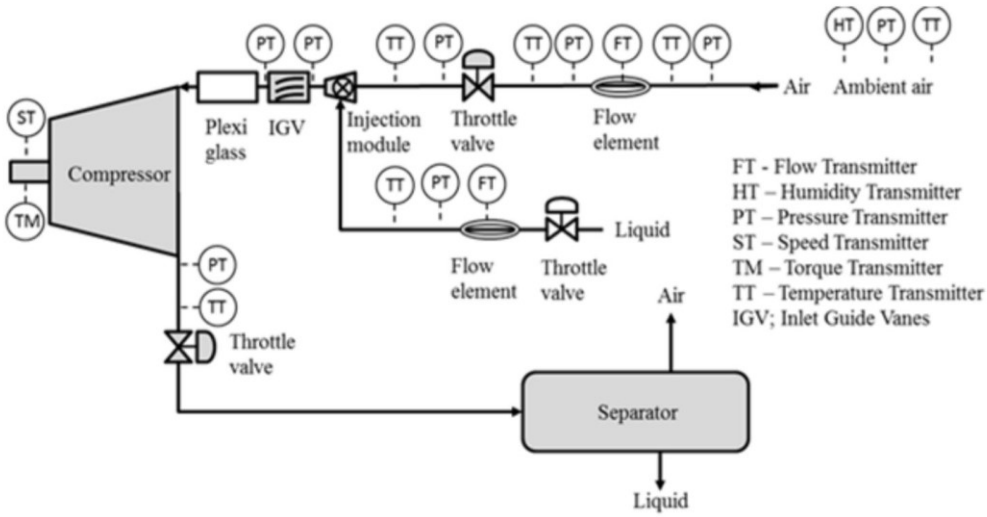

Figure 4.1: Test rig P&ID [27].

An overhung design with an axial inlet was used for the compressor section. However, a VIGV system could be assembled to control the inlet angle. The impeller was fixed to the shaft with a bearing pedestal, this was used to prevent water penetrating the electric motor. The bearing pedestal was connected to the electric motor through a torque meter, which provided accurate measurement of static and dynamic compressor power. Test rig operational conditions are presented in Table 4.1.

Table 4.1: Test rig operational range.

Description	Quantity
Suction conditions	Atmospheric
Test fluids	Air/water
Air-flow range	0-3 kg/s
Water-flow range	0-5 kg/s
GVF range	99.92-100%
GMF range	40-100%

The compression section was module based, making it easy to change between different impeller and diffuser designs. At the front of the impeller, four large PMMA windows provided visual access to the impeller outlet and different instrumentation was assembled radially. The diffuser was radially visible through the PMMA window in the section split. The compressor section is displayed in Figure 4.2

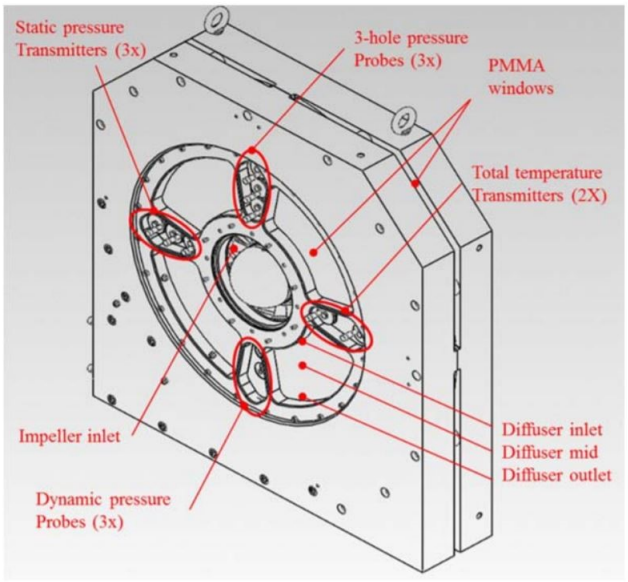

Figure 4.2: Compressor section with diffuser instrumentation [27].

The compressor was driven by a 450 kW electric motor with a maximum rotational speed of 1100 rpm. The speed could be regulated using a variable speed system. A discharge throttle controls the volume flow. Table 4.2 presents the main compressor data.

Table 4.2: Main compressor dimensions.

Description	Quantity
Inlet shroud diameter	250 mm
Inlet hub diameter	164.696 mm
Impeller outlet diameter (D_2)	400 mm
Impeller outlet blade height	19 mm
Outlet pipe diameter	200 mm

The water injection system consisted of 16 nozzles, equally distributed around the pipe wall. The nozzles were mounted at an inclined angle to the flow, the water was provided by a pump or the water grid. The pressure of the water can be operated between 0 and maximum 15 bars. Variation in nozzle size was utilized to achieve different droplet sizes. However, previous test has shown that the droplet size is not an important parameter when in wet gas performance, and that the droplets from the nozzles coalesce before the impeller inlet [27]. A pipe section in PMMA gave visual access to the compressor inlet, as depicted in Figure 4.3, here with the VIGV module fitted.

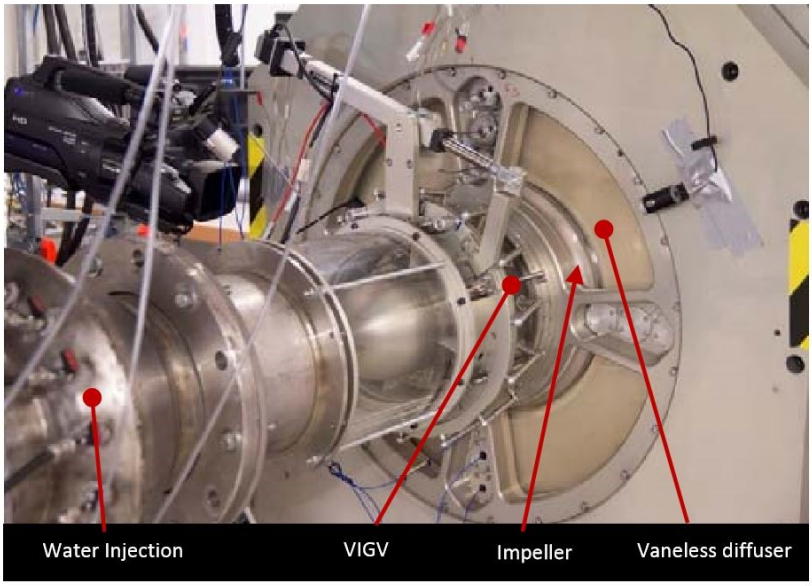

Figure 4.3: Compressor rig, with water injection system and VIGV module fitted [26].

The acquisition system for the test rig is the National Instruments PXI solution, which permits synchronous sampling up to 20 kHz. The instrumentation setup and performance testing were in accordance with ASME PTC-10 [27]. The accuracy of the instrumentation is presented in Table 4.3.

Table 4.3: Test rig instrumentation.

Instrument section	Accuracy	Unit
Ambient temperature	± 0.2	°C
Ambient pressure	± 0.15	hPa
Relative humidity	± 1	%
Temperature flow element	± 0.15	°C
Pressure diff. flow element	± 0.04	%
Dynamic pressure diffuser	0.14	mbar
Static pressure diffuser	± 0.002	bar
Total temperature diffusor	± 0.009	°C
Three hole prove diffusor	0.11	%
Inlet pressure compressor	± 0.3	%
Inlet temperature compressor	> ± 0.1	°C
Outlet pressure compressor	± 0.3	%
Outlet temperature compressor	> ± 0.1	°C
Water flow meter	± 0.5	%
Shaft speed	± 5	rpm
Shaft torque	± 0.48	%

4.2 Variable inlet guide vanes assembly

The VIGV assembly consisted of 14 curved blades, which could be turned by an actuator. The incidence angle was able to be operated between -25° and 42°. The VIGV assembly was mounted just upstream the impeller, and the guide vanes were surrounded by a transparent Plexiglas for visualization purposes. In Figure 4.4 the VIGV assembly is depicted.

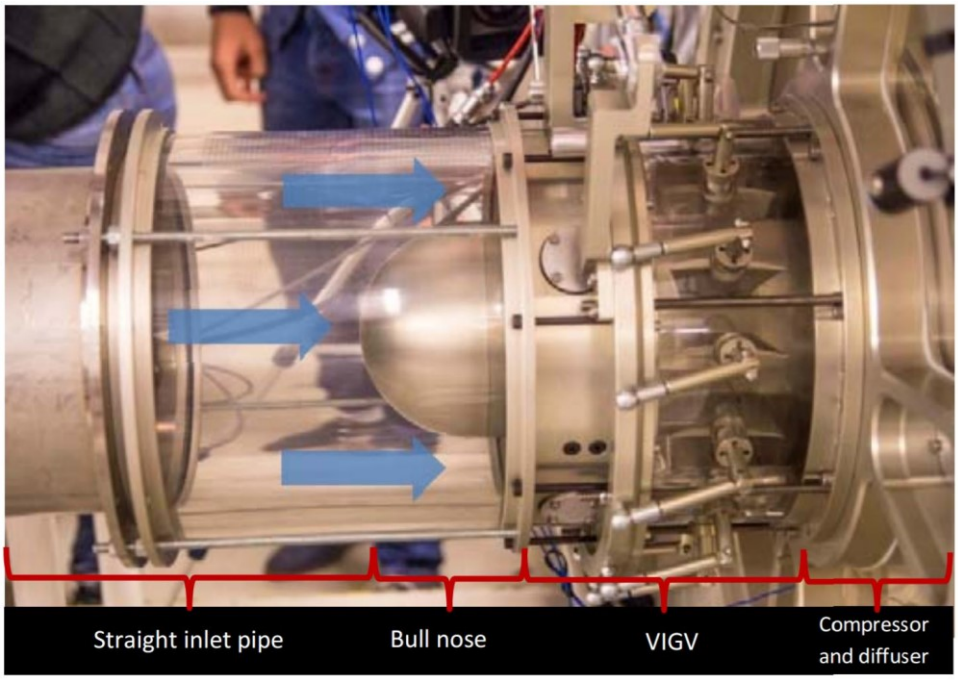

Figure 4.4: VIGV module configuration [26].

The vanes were designed with a twisted geometry and a deflection angle of 20° at root mean square (RMS), in the direction that gave prewhirl to the inlet of the compressor. The deflection angle changed over the radius with highest deflection at the tip and lowest at the hub. The geometry of a single guide vane is presented in Figure 4.5.

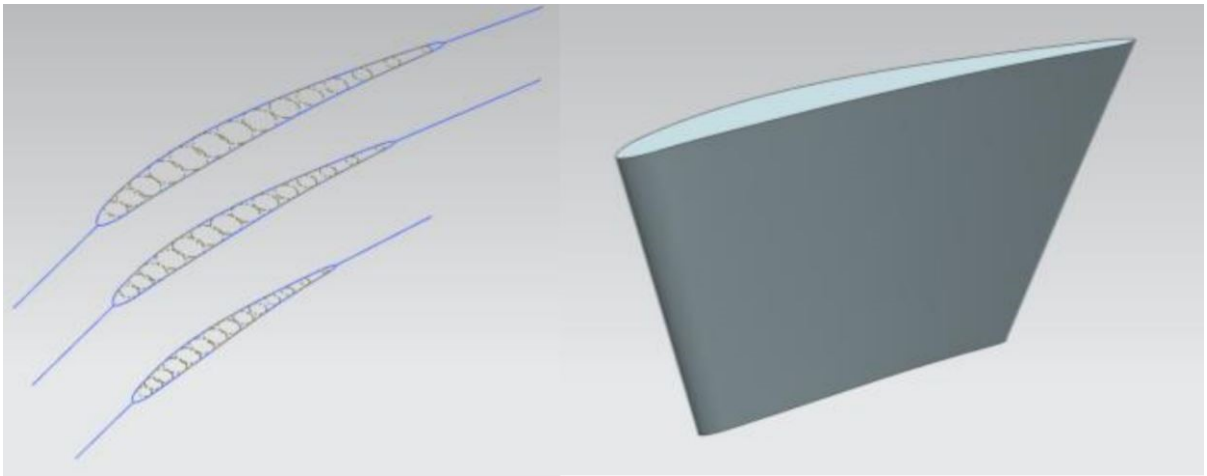

Figure 4.5: Guide vane geometry [28].

The blade chord increases from hub to tip and the design is based on the trade-off between desired angle play of VIGV and the desire of a gentle turning and better flow control. Table 4.4 presents the VIGV airfoil parameters.

Table 4.4: VIGV airfoil parameters.

Description	Symbol	Quantity
Pitch-cord ratio	p/c	0.7
Chamber angle RMS	θ	20 deg
Cord length RMS	c	67 mm
Maximum thickness RMS	t	5.3 mm
Point of maximum thickness	Xc/c	0.45
Point of maximum chamber	a	0.40
Aspect ratio	h/c	0.68

5. Experimental procedure

This chapter will present the experiments preformed to answer the given problem description in Chapter 1.1.

All tests were conducted with nozzle NF01 and NF06 with pressure provided by the water grid giving a droplet size of approximately 90 µm and 190 µm respectively. See nozzle data in Appendix B. The previous experiments at the NTNU test facility have indicated that droplet size had negligible effect on compressor performance [27].

5.1 Test 1: Validation of VIGV assembly function

Test 1 was preformed to validate that the VIGV assembly at the NTNU test facility performed according to theory. The test was first performed with dry gas and then with wet gas at different GMF.

The VIGV was tested at its maximum values, 42 degree prewhirl and -25 degree counter whirl. In addition, a refence point at 0 degree prewhirl was obtained. The impeller speed was kept constant at 9000 rpm and compressor discharge valve opening was kept constant at 55%. The test matrix is presented in Table 5.1.The position of the outlet valve was decided by starting close to design point ($Q = 1{,}2\ \mathrm{m^3/s}$) for dry gas at 0 degree prewhirl.

Table 5.1: Test 1, test matrix.

Outlet valve	GMF	Impeller theoretical inlet angle
Constant discharge valve opening	1.0	42° 0° -25°
	0.98	42° 0° -25°
	0.95	42° 0° -25°
	0.90	42° 0° -25°
	0.80	42° 0° -25°
	0.70	42° 0° -25°
	0.60	42° 0° -25°

The compressor discharge valve was kept constant to investigate how a compressor operating close to design point at dry conditions would react when the liquid content increases and especially how it affects the VIGV operating area. The expected results from this test can be seen in Figure 5.1, this is for the dry gas case. It is expected that reduced GMF will lead to an increase in pressure ratio and reduction in volume flow. The change in volume flow and pressure ratio at increased liquid content is highly dependent on relative location on the compressor map. At relatively high volume flow, it is expected that up-stream impeller eye pressure loss will increase significantly at wet conditions. This leads to a drop in impeller eye absolute pressure. Though the impeller eye volume flow would remain the same, the location of the inlet flow meter will give lower mass and volume measurements.

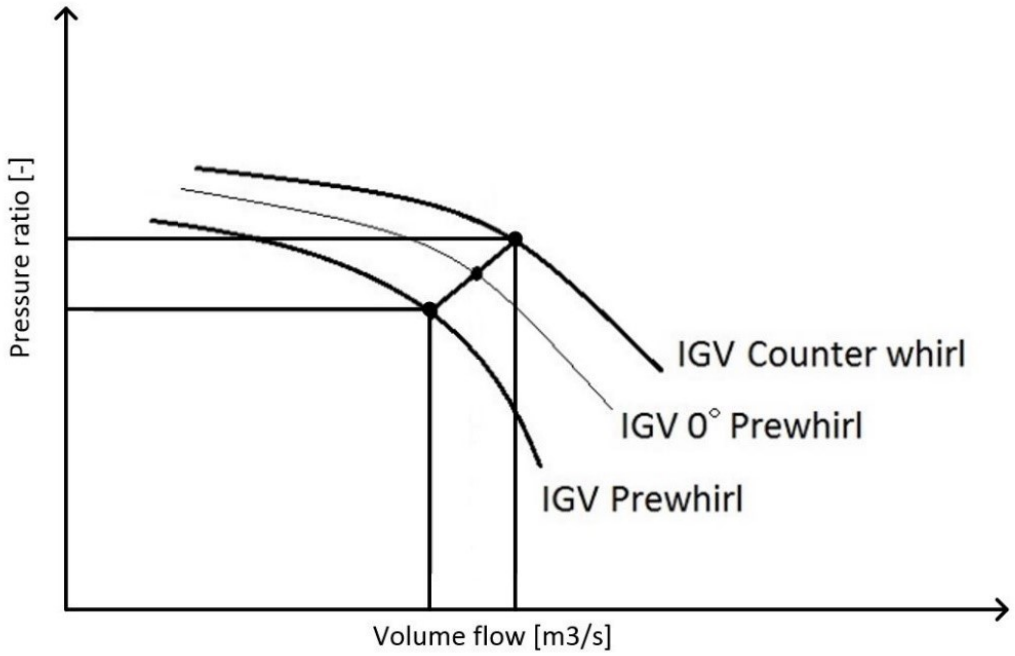

Figure 5.1: Anticipated result from test 1.

5.2 Test 2: Comparing VIGV with VSD

The main object for test 2 was to investigate if the VIGV and VSD had the same impact on compressor performance. The test was performed with dry gas only and the outlet valve was set to the same position as for test 1.

To show the VIGV's operating range, the impeller inlet angle was slowly changed from maximum prewhirl to maximum counter whirl while the engine speed was kept constant at 9000 rpm. For the VSD, the IGV was set to give 0 degree prewhirl and the engine speed was slowly changed from 8000 to 10000 rpm.

The expected results from the VSD test can be seen in Figure 5.2, for the VIGV the results will be the similar as for test 1. It is interesting to see how the VSD will perform compared to the VIGV.

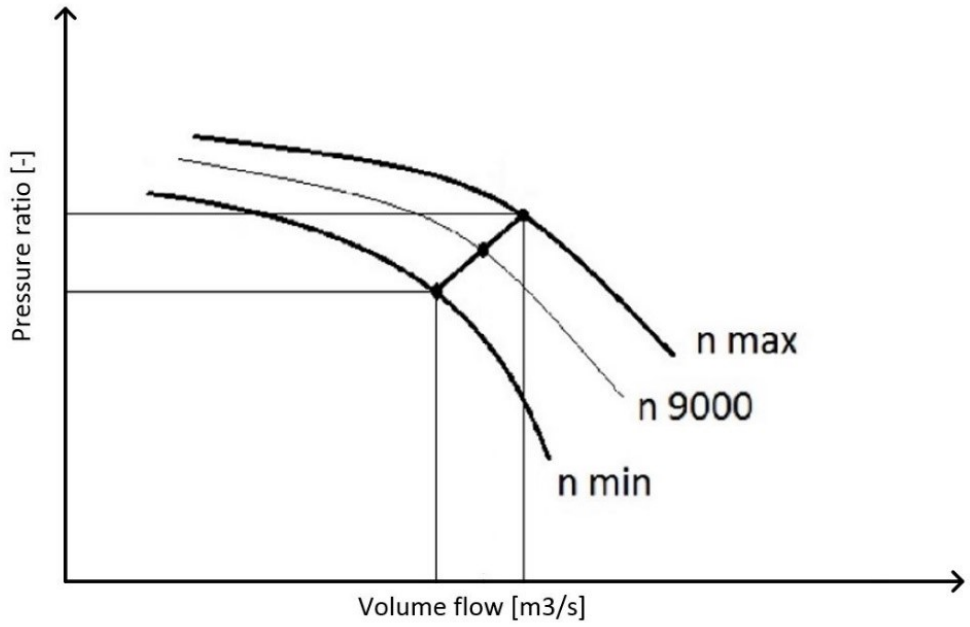

Figure 5.2: Anticipated results from test 2.

5.3 Test 3: Establishing maximum and minimum values

The aim for test 3 was to find an area in the compressor map where the compressor could be operated independent of liquid content by changing the VIGV and the outlet valve. To find this area four curves were needed, two for dry gas and two for wet gas. The two curves for each case were obtained with the IGV positioned at maximum prewhirl and maximum counter whirl.

The dry curves were recorded continuously while slowly closing the opening valve. For the wet curves, this could not be done since GMF changes with varying volume flow, instead seven points were logged for each curve.

Originally it was planned to run the wet gas case with a very high liquid content to explore the maximum values. However, with high liquid content the operation range becomes very narrow and therefore the wet gas case was performed at GMF 0.7. The anticipated results can be seen in Figure 5.3.

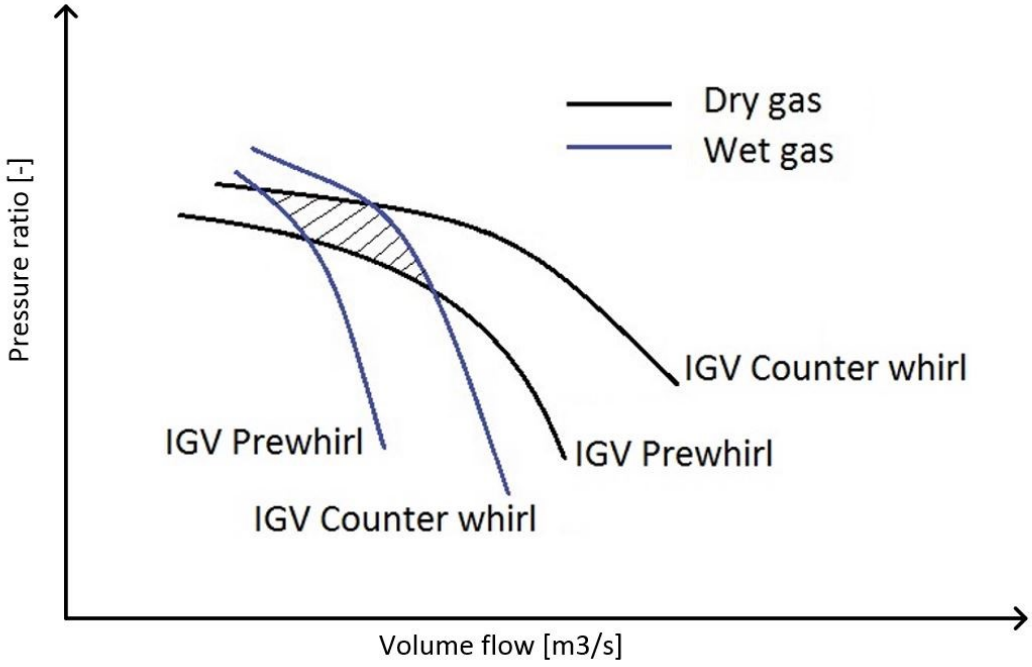

Figure 5.3: Anticipated results from test 3.

5.4 Test 4: Slug testing

Test 4 was performed to investigate how a compressor operating at design point with dry gas would react to increased liquid content and how it would be possible to keep the same pressure ratio and volume flow by adjusting VIGV and outlet valve. The engine speed was kept constant at 9000 rpm. The test was performed following sequence below and as indicated in Figure 5.4:

1. Stable operation at point 1, with dry gas and 12 degree prewhirl. Some prewhirl in the initial position to be able to raise the performance.
2. Increasing the liquid content to point 2, with a new volume flow and pressure ratio.
3. VIGV and outlet valve was adjusted to bring the compressor back to operation point 1.
4. Decreasing the liquid content back to dry gas. This causes the compressor to go to a operation point 3 in Figure 4.3.
5. Adjusting the VIGV and outlet valve back to their original positions, this returns the compressor performance back to operation point 1.

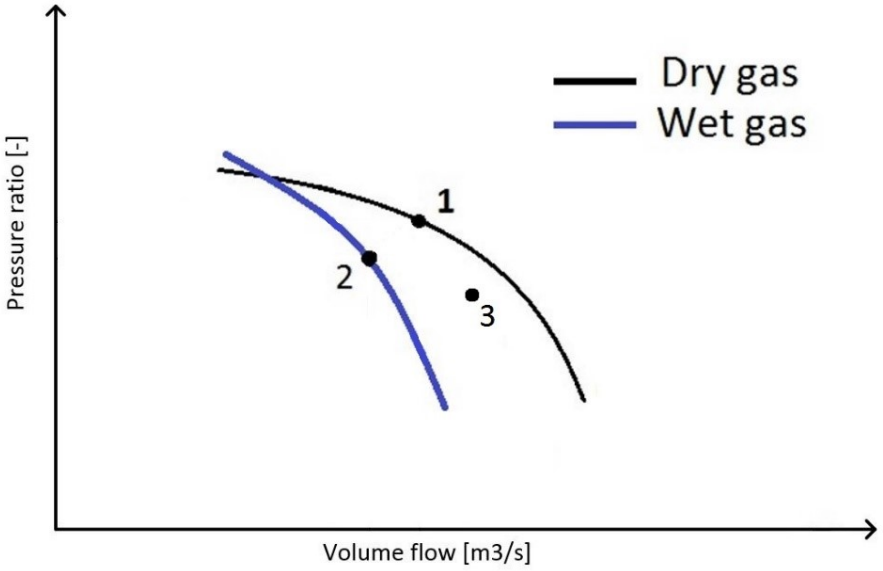

Figure 5.4: Anticipated results from test 4.

The test was repeated with three wet gas cases ranging from GMF 0.9 to GMF 0.7. This test was conducted to show that VIGV can be used to compensate for varying wet gas conditions.

5.5 Post processing

The NTNU test facility produces spread sheet records with all the different test parameters. Since the results in this report was mostly focusing on pressure ratio rather than polytropic head or efficiency, post processing mainly consisted of simple calculations. During testing, relevant instrumentation was monitored to achieve stable conditions for every test point. Each point presented in the results is an average over a given time. Except from the dry curves in test 3 and the results from test 4 since these were recorded continuously. Recording was done with a sample rate of 2 Hz. Compressor inlet volume flow and GMF was calculated and recorded directly by the National Instruments PXI used for control and monitor for the compressor test rig.

6. Results and discussion

This chapter will present and discuss the results obtained from the experiments presented in the Chapter 5. The results will mainly be presented with focus on pressure ratio and volume flow.

The main objective of test 1 was to validate that the VIGV assembly functions according to theory. The experimental results can be found in Figure 6.1. Three points where recorded at each GMF; maximum prewhirl, zero prewhirl and maximum counter whirl. The results show that operating area for prewhirl was significantly larger than for counter whirl. This can be seen as the interval between maximum prewhirl and zero prewhirl were larger than the interval between maximum counter whirl and zero prewhirl.

As expected, with increasing liquid content the pressure ratio war increased and the volume flow was decreased. An interesting result is that for GMF 0.60, maximum counter whirl gave a lower performance than for zero prewhirl. This means that the VIGV chokes the flow at these conditions.

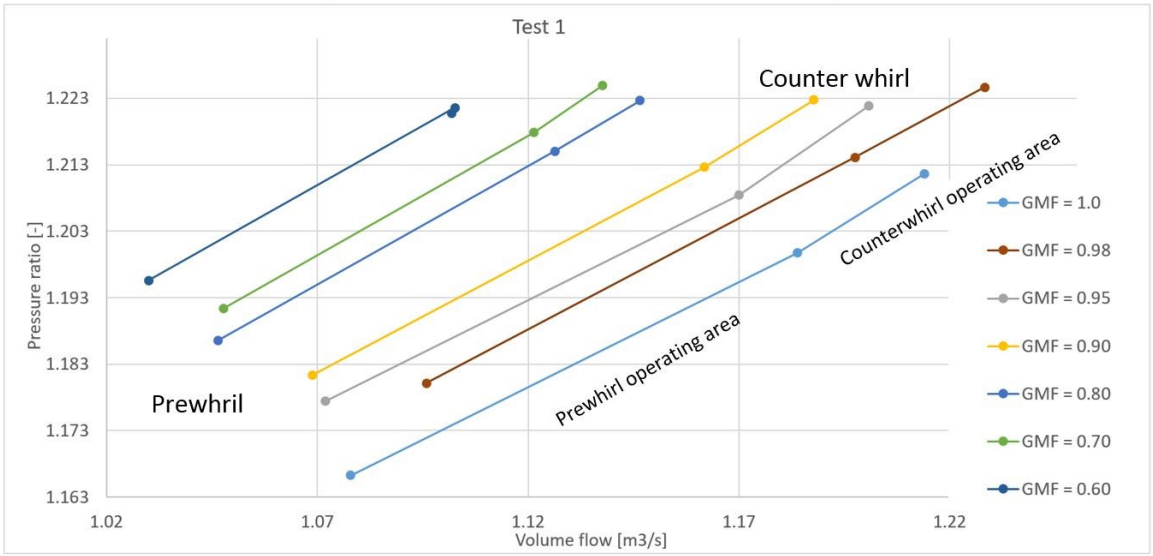

Figure 6.1: Maximum prewhirl, zero prewhirl and maximum counter whirl at various GMF.

There was a significant jump between the dry gas case and GMF 0.98, see red line in Figure 6.1. The increased pressure ratio was expected due to increased density and this has been well documented in previous test campaigns, see Chapter 2.5.2. However, the increase in volume flow was unexpected. A possible explanation is that the liquid evaporative cooling of the inlet and outlet air was a significant factor at low liquid content. The reduced temperature at impeller inlet increased the gas phase density which will caused an increased volume flow at the inlet flow meter with the same impeller eye volume flow. The reduced temperature and increased outlet pressure caused an increased compressor outlet density. This will reduce the discharge valve restriction allowing for higher compressor inlet flow.

When the liquid content was increased, the pressure ratio increased even further whiles the volume flow decreased. The decrease in volume flow can be explained by increased boundary layers and momentum losses that contribute to an increased blockage in the flow.

The jump between GMF 0.90 and GMF 0.80 was somewhat more unclear. A possible explanation is that there was a shift in the flow direction in the volute. A shift would cause a change in compressor performance, this phenomenon may be documented in future works.

The predicted decrease in VIGV effect on volume flow and pressure ratio with increasing liquid content was experienced. To highlight the decrease, the ratio between maximum and minimum volume flow and pressure ratio was calculated according to Equation 6.1 and 6.2.

$$\hat{\pi} = \frac{\pi_{-25°}}{\pi_{42°}} \tag{6.1}$$

$$\hat{Q} = \frac{Q_{-25°}}{Q_{42°}} \tag{6.2}$$

The VIGV relative effect on volume flow and pressure ratio is shown against GMF in Figure 6.2. It is evident that the VIGV effect on volume flow was reduced more than its effect on pressure ratio. For volume flow, there was a significant reduction in the VIGV effect from 12.6% at dry condition to 7.1% at GMF 0.60. The pressure ratio changes from 3.9% at dry conditions to 2.2% at GMF 0.60. This is similar to what Vigdal reported et al [26],

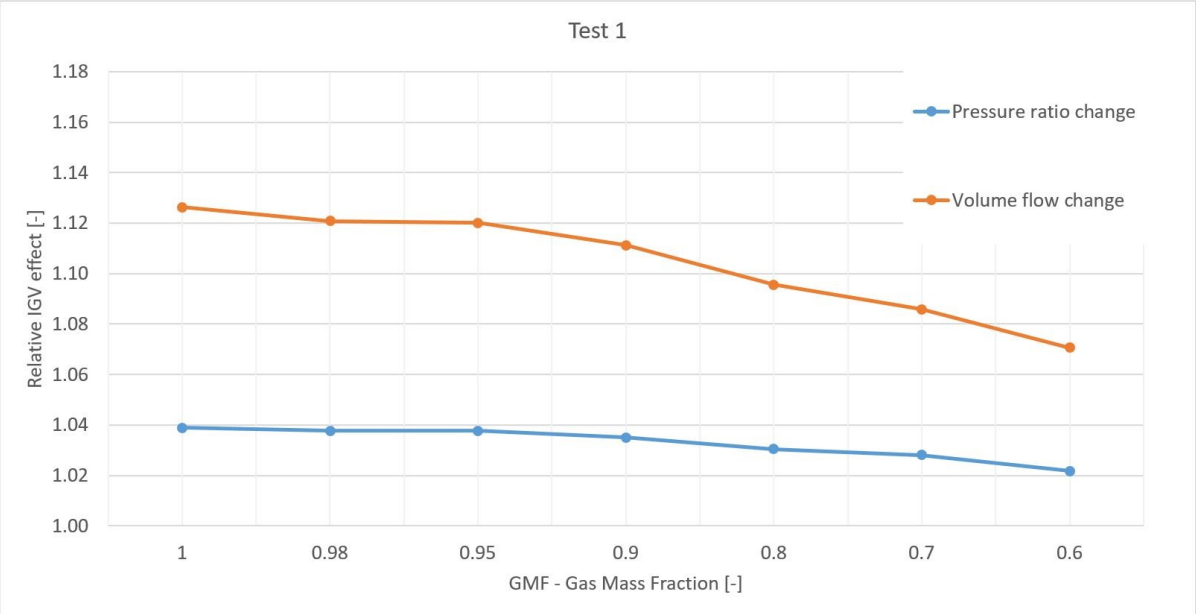

Figure 6.2: VIGV effect on the compressor with liquid content up to GMF 0.6.

As Vigdal [26] concludes, a large contributor to the reduced VIGV effect is increased momentum transfer between liquid and gaseous phases. With increasing liquid content the guide vanes ability to direct the flow of liquid decreases. To have a water droplet perfectly follow the gas flow (St=1), the droplet size needs to be 5-10 µm [26] and the smallest droplet size currently possible at the test facility was 70 µm. Increased liquid content leads to a larger degree of droplet-to-droplet interaction and coalescence. In addition, Ober et al [29] showed that increased liquid content (down to GMF 0.979) leaded to reduced deflection. Since the deflection of droplets is smaller than for the gas, the deflection of gas is reduced with increased liquid content. For the VIGV, this means that although the theoretical whirl is the same for all cases, the actual inlet whirl angle for the impeller is reduced with increasing liquid content.

It should also be mentioned that the decrease in VIGV performance is not entirely due to increased liquid content. The reduced volume flow gives typically a reduced effect VIGV performance regarding pressure ratio and volume flow at dry conditions.

The main objective for test 2 was to compare the performance of VIGV and VSD. The results can have been plotted in Figure 6.3. The pressure ratio is plotted against the volume flow, the performance of VSD lies closely to the performance of VIGV. This shows that these two methods have the same effect on compressor performance, although the operating area for VSD is larger than for VIGV. To achieve the same operating area considering volume flow and pressure ratio the engine speed had to be changed from 8220 to 9220 rpm. The VIGV was changed from 42° prewhirl to -25° counter whirl at the selected initial compressor operational point.

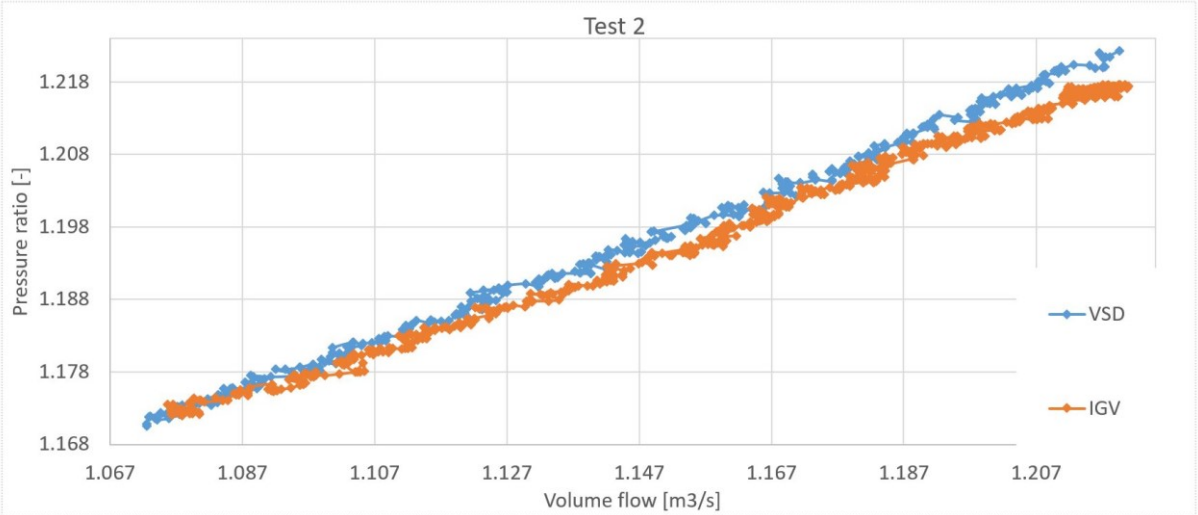

Figure 6.3: Comparison of compressor performance with VSD and VIGV.

The torque is displayed against the volume flow in Figure 6.4. At low volume flow the torque for VIGV was lower than the torque for VSD. At approximately 1.18 m^3/s there was a shift and the torque for VIGV became higher for greater volume flow. The shift happens when the prewhirl provided by the VIGV was zero. At this point the two cases had the same settings regarding VIGV angle and engine speed. The line for VSD is more uneven due to the fact that the speed was increased 20 rpms each step whereas the VIGV was slowly changed from maximum prewhirl to maximum counter whirl.

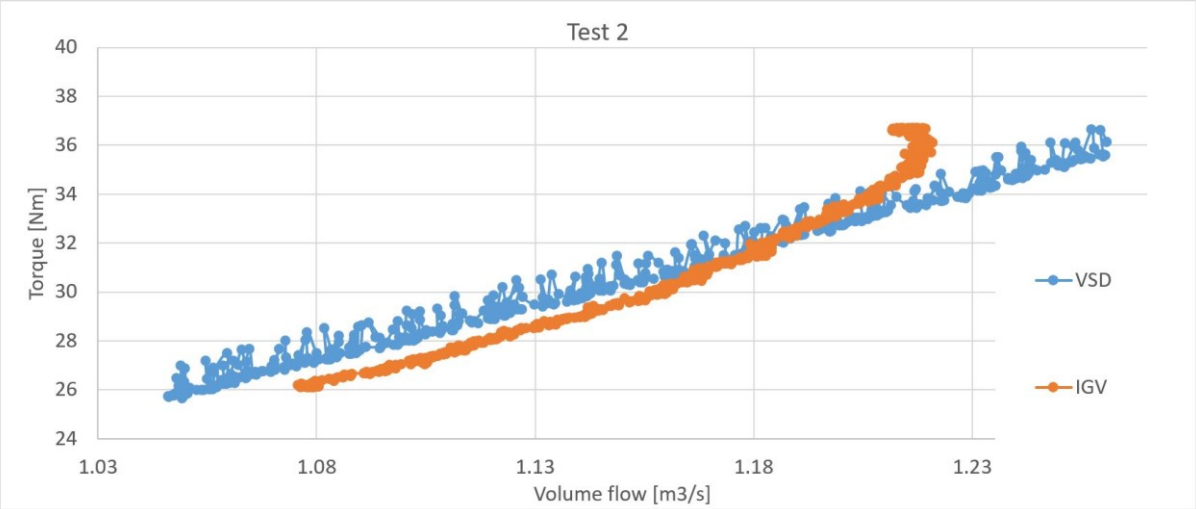

Figure 6.4: Comparison of torque between VSD and VIGV.

By combining these two graphs from test 2 it is possible to say that the VIGV performs well in comparison to VSD in the prewhirl area. When it comes to counter whirl however, the increase in torque without an increase in performance implies an overall loss in compressor efficiency.

The head represented by the shaft torque increases. It is expected that head to parasitic losses remains the same between VIGV and VSD. As difference in pressure ratio between VSD and VIGV is small, it is obvious that be the use of VIGV, a higher head is required to produce the same pressure ratio at counter whirl. Hence, an overall loss in efficiency with VIGV at counter whirl is experienced.

Test 3 was conducted to find an area where the compressor could be operated independently of liquid content by changing the angle of the VIGV and the compressor outlet valve. The result can be seen in Figure 6.5. On the contrary to the expected result that that is presented in Figure 5.3, the compressor curve for GMF 0.7 lies quite close to the compressor curve for the dry gas case. In the area between the two curves for GMF 0.7, the compressor can be operated with the liquid content ranging from dry to GMF 0.7.

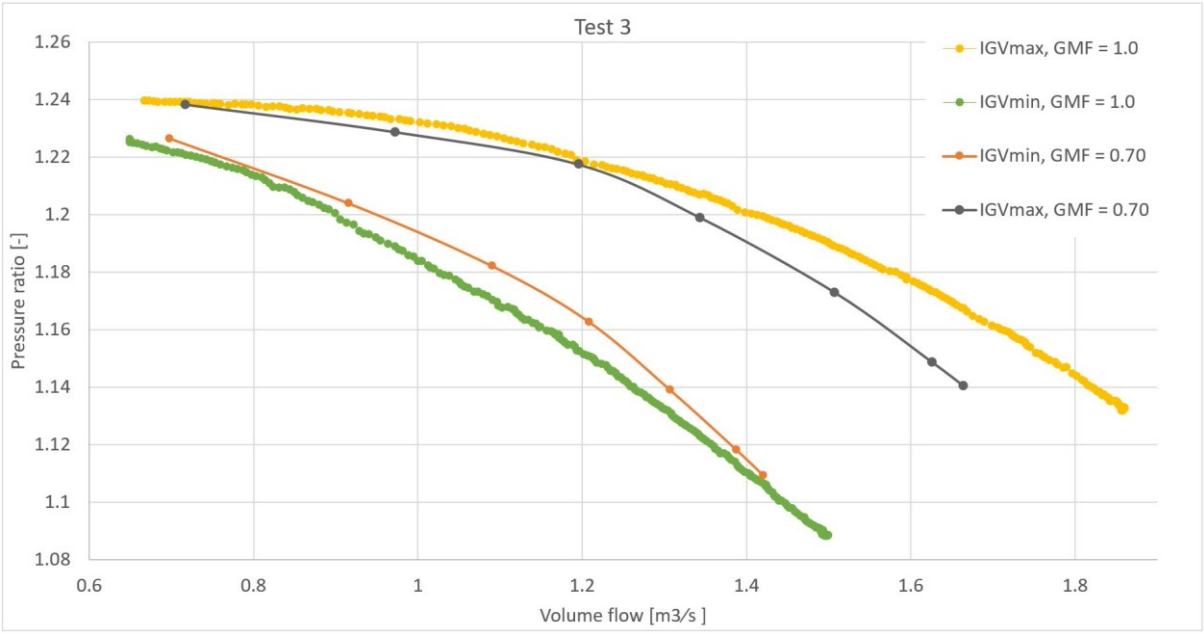

Figure 6.5: Compressor curves for GMF 1.0 and 0.7 with VIGV angle where min and max refer to maximum prewhirl and maximum counter whirl respectively.

The performance for GMF 0.7 lies remarkably close the dry gas, especially compared to the results published by Bertoneri [13], see Figure 2.10. The difference between LVF 1% (GMF = 0.69) and LVF 0% (GMF = 1.0), especially at high volume flow, distinguish these results. However, when compared to the results published by Ferrara [14], see Figure 2.12, the slope of the GMF 0.7 curves was more similar. There seems to be and a difference between the compressor that Bertoneri used and the one at the NTNU test facility. One significant difference is that the compressor Bertoneri used has a larger and curved distance between the impeller and the diffuser. This makes it more exposed to pressure losses due to water-wall splashing and liquid-gas drag forces. In addition, Bertoneri's test campaign differs by having fixed IGV, closed loop and higher inlet pressure. The only difference to Ferrara's test campaign was that the VIGV assembly was not fitted.

It was expected that increased liquid would result in higher derivatives, but lower GMFs results in a narrow operating area and test 1 showed that the VIGV performance decreases. This indicates that if this test was to be performed with a lower GMF, the area where the compressor could be operated independently of the liquid content, would become smaller and more like the anticipated result.

The main objective with test 4 was to investigate how the compressor would react to an increased liquid content, and how it would be possible to keep the volume flow and pressure ratio constant by adjusting the inlet prewhirl and the outlet valve. This was done by changing from dry gas to three different GMFs and back again to dry.

Figure 6.6 shows how the compressor reacted when the liquid content changed from dry to GMF 0.9. The initial position was at pressure ratio and volume flow equal to 1.2. When the water was injected, the volume flow quickly decreased and the pressure ratio increased. Then the compressor performance was adjusted back to initial position by changing the outlet valve and VIGV angle. When the water was closed off, the volume flow quickly increased and the pressure ratio decreased. Then it was adjusted back to the initial position again.

To follow the procedure in the compressor map, the steps are numbered. (1) Starting point, (2) liquid injected, (3) VIGV adjusted, (4) outlet valve adjusted, back at initial point, (5) liquid stopped, (6) VIGV adjusted and (7) outlet valve adjusted, back at initial point.

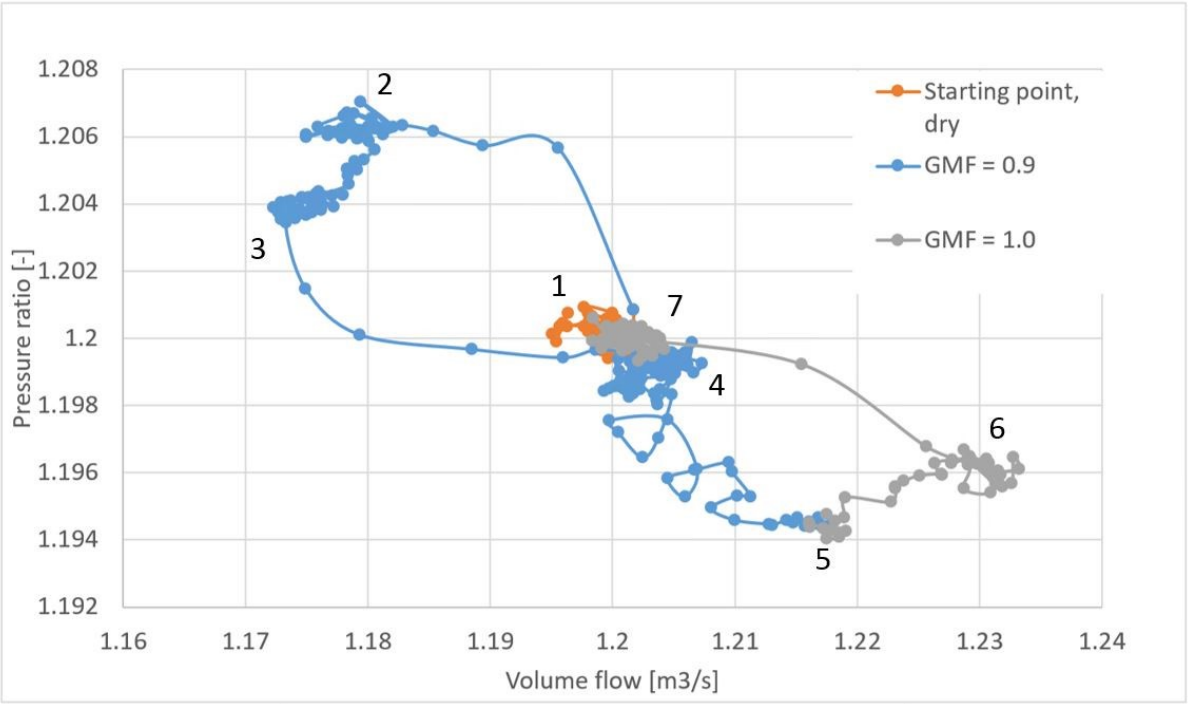

Figure 6.6: From dry to GMF 0.9.

Higher water content resulted in larger variations in pressure ratio and volume flow. The performance was varying in the same order in all the cases. The results for a slug at GMF 0.8 is presented in Figure 6.7. How varying the IGV angle effect the performance is more unclear in this case than with GMF 0.9. Because the VIGV was adjusted less, most of the adjustment required to obtain the initial position was obtained by adjusting the outlet valve.

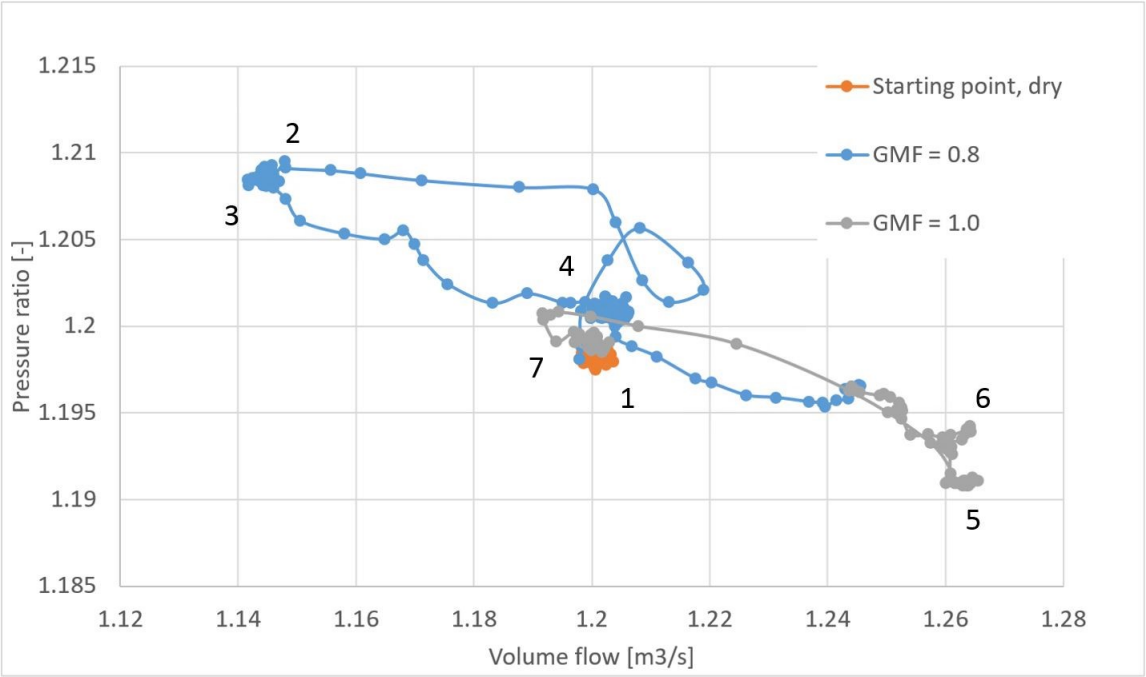

Figure 6.7: From dry to GMF 0.8.

For both the GMF 0.9 and 0.8 cases, the VIGV was used to lower the performance curve. For GMF 0.7 however, the VIGV was used to lift the curve, this can be seen as point 2 is lower than point 3 unlike the other cases. The results from this case can be seen in Figure 6.8.

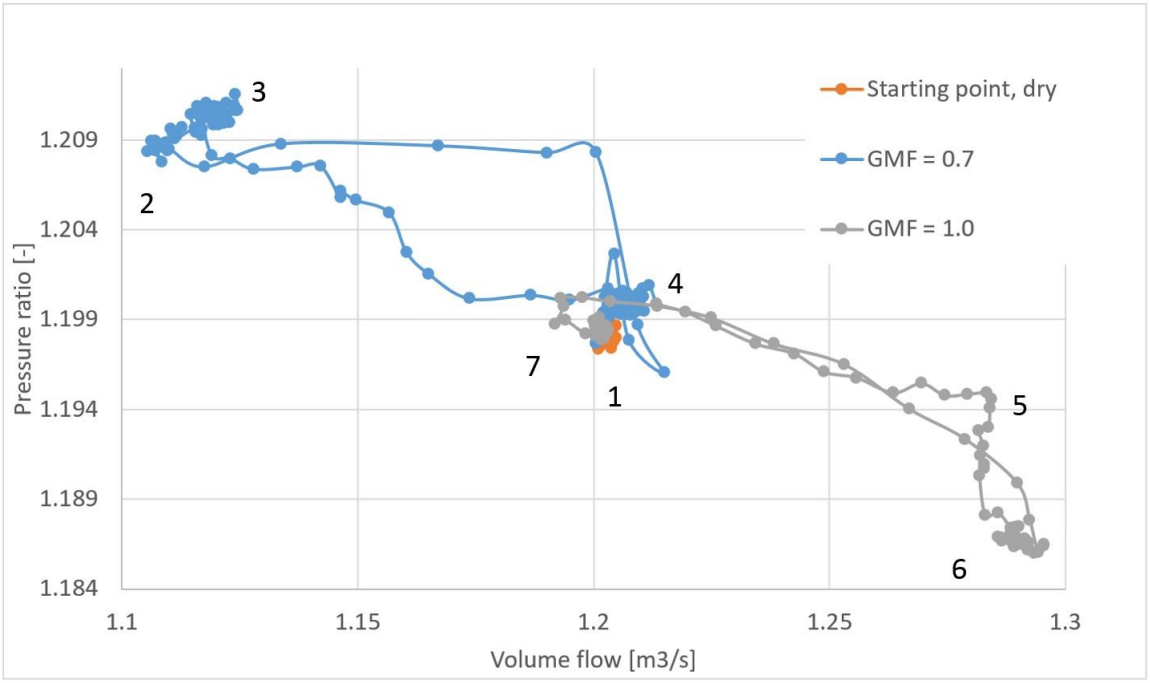

Figure 6.8: From dry to GMF 0.7.

How much the VIGV was adjusted in the different cases can be seen in Figure 6.9. The initial position was at 12 degree prewhirl. As mentioned above, only for GMF 0.7 the VIGV was used to lift the performance by giving less prewhirl. For GMF 0.9 and GMF 0.8 it was used to lower the performance by giving more prewhirl.

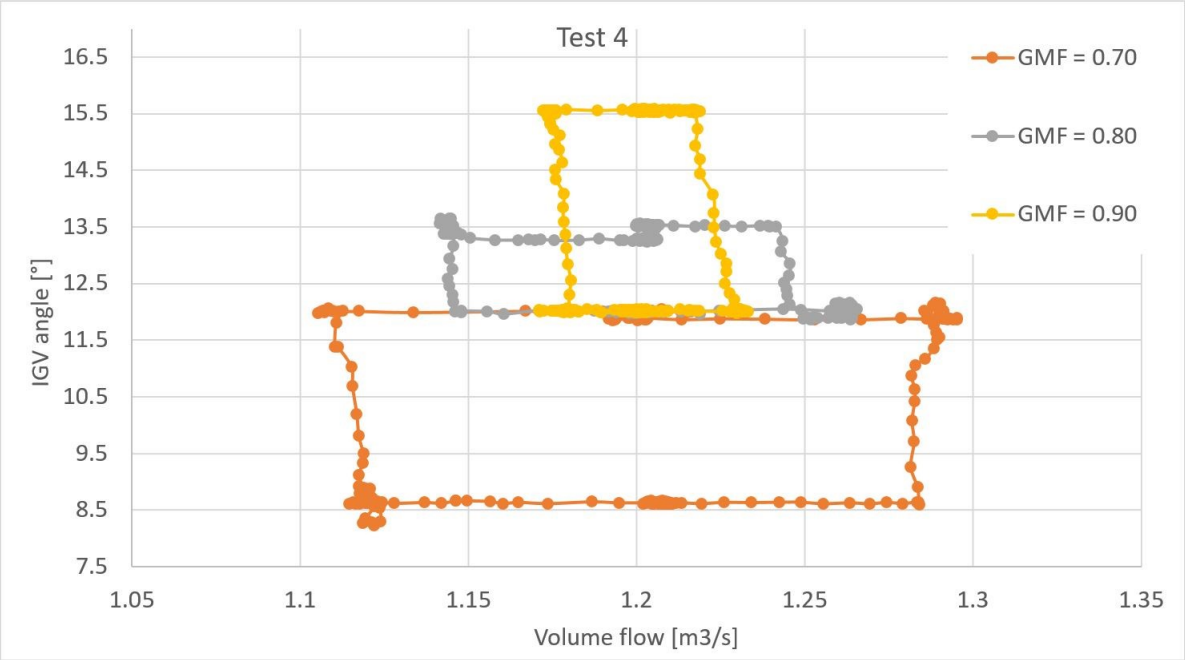

Figure 6.9: VIGV angle adjustment for the different cases.

Although the VIGV was used to achieve the initial pressure ratio and volume flow, it was more dependent on changing the outlet valve. It seems like injecting liquid have similar effect on pressure ratio and volume flow as changing the outlet valve. This indicates that significant amount of the effect seen when injecting liquid is due to increased blockage of the impeller downstream area. Most likely a significant change in the discharge coefficient of the compressor discharge valve. Through this test the VIGV has shown that it is a valuable and quick instrument to adjust the compressor performance when the inlet liquid content changes.

7. Conclusion

A variable inlet guide vanes system has been examined in combination with a single stage centrifugal compressor. The main objective was to assess the influence wet gas has on the VIGV performance, how VIGV performs compared to variable speed drive (VSD) and how the VIGV could be utilized to keep stable compressor performance with varying liquid content. Four different test have been conducted at the NTNU test facility.

VIGV performance has been studied at the following gas mass fractions (GMF); 1.0, 0.98, 0.95, 0.90, 0.80, 0.70 and 0.60. For each of the different values of GMF, the compressor performance was recorded, while the VIGV angle was changed from maximum prewhirl to maximum counter whirl. These experiments resulted in the following findings:

- The VIGV effect on pressure ratio and volume flow declines with increasing liquid content. This is due to the increased momentum transfer between liquid and gaseous phases.
- Increasing liquid content correlated with increased pressure ratio and reduced volume flow. With one exception at GMF 0.98, the pressure ratio and the volume flow increased compared to the dry gas cases.
- The performance of VIGV compared to the performance of VSD differed little with respect to both volume flow and pressure ratio.
- When the VIGV provided counter whirl the overall efficiency of the compressor decreased compared to the VSD controlled compressor case.

To show that the VIGV could be used to keep stable compressor performance with varying liquid content, the inlet composition was changed from dry gas to the following GMF; 0.9, 0.8 and 0.7. The VIGV and the outlet valve were used to keep the same pressure ratio and volume flow independent of liquid content. For GMF 0.9 and GMF 0.8 the VIGV was used to lower the compressor performance by inducing prewhirl. While for GMF 0.7 the compressor performance was increased by inducing less prewhirl. The maximum change in VIGV angle needed was 3.5°.

Utilization of VIGV was demonstrated as an efficient method to adjust the compressor performance with varying inlet liquid conditions, even though the VIGV effect on pressure ratio and volume flow decreased with increasing liquid content.

7.1 Further work

Based on literature review and experimental results, further work should be focused on the following subjects:

- Reducing the Stoke number by either smaller droplets or substitute water with a suitable fluid.
- Investigate the difference between the VIGV angle and the impeller inlet angle.
- Comparing VIGV to VSD with wet gas flow.

References

[1] Oil and gas production. 2017. Retrieved May 15, 2017, from http://www.norskpetroleum.no/en/production-and-exports/oil-and-gas-production/

[2] Brenne, L.. Bjørge, T., 2008, Prospects for subsea wet gas compression, Proceedings of GT2008, Asme turbo 2008, Berlin, Germany.

[3] Henriksen, M., 2016, Wet gas compression – inlet guide vanes, NTNU, project thesis.

[4] Saravanumutto, H., Cohen, H. Rogers, G., 2001, Gas turbine theory, 5^{th} edition, Pearson Education Ltd.

[5] Hundseid, Ø., 2008, Evaluation of Performance Models for wet gas Compressors, Trondheim, Norway.

[6] Bakken, L. E., Thermodynamics Compression and Expansion Processes, NTNU. Handout in the course TEP04 – Gas Turbines and compressors, Fall 2016.

[7] Schultz, J. M., 1962, The polytropic Analysis of Centrifugal Compressors, Journal of Engineering for Power.

[8] Hundseid, Ø., 2006, Wet gas performance analysis, Proceedings of GT2006, ASME Turbo Expo 2006, Barcelona, Spain.

[9] Grüner, T., Bakken, L. E., 2011, Aerodynamic instability investigation of centrifugal compressor exposed to wet gas, 9th European conference on Turbomachinery,

[10] Rezkallah &Zhao, 1995, Validated the theory of flow pattern related to the Weber number in microgravity.

[11] Centrifugal Compressor. 2015. Retrieved March 9, 2017, from http://petrowiki.org/Centrifugal_compressor

[12] Hundseid, O., et al, 2008, Wet Gas Performance of a Single Stage Centrifugal Compressor, Proc. ASME IGTI Turbo Expo (New York, NY: ASME 2008).

[13] Bertoneri, M., Wilcox, M., Toni, L., Beck, G., 2014, Development of test stand for measuring aerodynamic, erosion, and rotordynamic performance of a centrifugal compressor under wet gas condition, Proc. ASME Turbo Expo 2014, Düsseldorf, Germany.

[14] Ferrara, V., 2016, Wet Gas Compressors – Stability and Range. Trondheim, Norway.

[15] Inlet guide vanes control. Retrieved March 10, 2017 from http://www.damper-designs.co.uk/ivc.html

[16] Händel, D., Niehus, R., Rockstroh, U., 2006, Aerodynamic investigation of a variable inlet guide vane with symmetric profile, Proceedings of GT2006, ASME Turbo Expo 2006, Barcelona, Spain.

[17] Lampert, P., 2009, Investigation of endwall flows and losses in axial turbines. Part II. The effects of geometrical and flow parameters, Journal of theoretical and applied mechanics, Warsaw, Poland.

[18] Mechanical Engineering: Whats the difference between compressor surge and stall?. (2014). Retrieved March 22, 2017, from https://www.quora.com/Mechanical-Engineering-Whats-the-difference-between-compressor-surge-and-stall-1

[19] Cumpsty, N.A., 2004, Compressor aerodynamics, Malabar, Florida

[20] Coppinger, M., Swain, E., 1999, Performance prediction of an industrial centrifugal compressor inlet guide vane system, Proceedings of the institution of Mechanical Engineers, Leicestershire, UK.

[21] Nisenfeld, A.E., Centrifugal compressors, Principle of operation and control, 3^{rd} edition.

[22] Lüdtke, K. H., 2004, Process Centrifugal Compressors, Berlin, Germany.

[23] Grüner, T, Bakken, L. E., Brenne, L., Bjørge, T., 2008, An experimental investigation of airfoil performance in wet gas, Proceedings of ASME Turbo Expo 2008, Berlin, Germany.
[24] Ulrichs, E., Joos, F., 2006, Experimental investigation of the influence of water droplets in compressor cascade, Proceedings of GT2006 ASME Turbo Expo 2006, Barcelona, Spain.
[25] Grüner, T. G., 2012, Instability characteristic of a single-stage centrifugal compressor exposed to dry and wet gas, Proceedings of ASME Turbo Expo 2012,
[26] Vigdal, L. B., Bakken, L. E., 2016, Variable inlet guide vane effect on centrifugal compressor performance in wet gas flow, Proceedings of GT2016 ASME Turbo Expo 2016, Seoul, South Korea.
[27] Hundseid, Ø., Bakken, L. E., 2015, Integrated wet gas compressor test facility, Proceedings of GT2015 ASME Turbo Expo 2015, Montréal, Canada
[28] Vigdal, L. B., Bakken, L. E., 2015, Inlet guide vane performance at dry and wet gas conditons, Proceedings of GT2015 ASME Turbo Expo 2015, Montréal, Canada
[29] Ober, B., Joos, F., 2014, Experimental Investigation on Aerodynamic Behaviour of a Compressor Cascade in Droplet Laden Flow, ASME Journal of Turbomachinery 2014.
[30] Unpublished by producer BETE, can be provided upon request.

Appendix A – Risk assessment

NTNU	Hazardous activity identification process	Prepared by	Number	Date
		HSE section	HMSRV2601E	09.01.2013
		Approved by		Replaces
HSE		The Rector		01.12.2006

Unit: Department of Energy and Process Engineering **Date:**

Line manager: Olav Bolland

Participants in the identification process (including their function)**:** Rig responsible Erik Langørgen and student Martin Henriksen.

Short description of the main activity/main process: Master project for student Martin Henriksen. Wet gas compression – IGV control.

Is the project work purely theoretical? (YES/NO): NO *Answer "YES" implies that supervisor is assured that no activities requiring risk assessment are involved in the work. If YES, briefly describe the activities below. The risk assessment form need not be filled out.*

Signatures: *Responsible supervisor:* *Student:*

ID nr.	Activity/process	Responsible person	Existing documentation	Existing safety measures	Laws, regulations etc.	Comment
1	Compressor experiments dry and stable, changing IGV angle.	Erik Langørgen	Risk Assesment Report	Procedure for Running Experiments	The Work Enviroment Act	Operating in unstable conditions is not explicitly covered in Procedure for Running Experiments.
2	Compressor experiments dry and unstable, changing engine speed.					
3	Compressor experiments wet and stable, changing IGV angle.					
4	Compressor experiments wet and unstable, changing liquid content, IGV angle and outlet valve					

NTNU	Risk assessment	Prepared by	Number	Date	
		HSE section	HMSRV2603E	04.02.2011	
HSE/KS		Approved by		Replaces	
		The Rector		01.12.2006	

Unit: *Department of Energy and Process Engineering* **Date:**

Line manager: Olav Bolland

Participants in the identification process (including their function)**:** Rig responsible Erik Langørgen and student Martin Henriksen.

Short description of the main activity/main process: Master project for student Martin Henriksen. Wet gas compression – IGV control.

Signatures: *Responsible supervisor:* *Student:*

Activity from the identification process form	Potential undesirable incident/strain	Likelihood:	Consequence:			Risk Value (human)	Comments/status Suggested measures
		Likelihood (1-5)	Human (A-E)	Environment (A-E)	Economy/ material (A-E)		
1-4	Loss of hearing and/or eyesight.	1	D	A	A	D1	Wear hearing protection and safety glasses.
1-4	Thermal or mechanical fatigue. Parts may detach, enter the rotating impeller and get flung out.	1	D	A	D	D1	Gradually decrese flow. Check inlet before start for lose parts. Start slowly monitoring temperatures and mechanical stability. Avoid standing on the side of the impeller. Closed from unathorized personnel
4	Rapid increase of load. Risk of mechanical failure.	1	D	A	D	D1	Start with small increase of load, gradually increase.

Likelihood, e.g.:
1. *Minimal*
2. *Low*
3. *Medium*
4. *High*
5. *Very high*

Consequence, e.g.:
A. *Safe*
B. *Relatively safe*
C. *Dangerous*
D. *Critical*
E. *Very critical*

Risk value (each one to be estimated separately):
Human = Likelihood x Human Consequence
Environmental = Likelihood x Environmental consequence
Financial/material = Likelihood x Consequence for Economy/materiel

Potential undesirable incident/strain

Identify possible incidents and conditions that may lead to situations that pose a hazard to people, the environment and any materiel/equipment involved.

Criteria for the assessment of likelihood and consequence in relation to fieldwork

Each activity is assessed according to a worst-case scenario. Likelihood and consequence are to be assessed separately for each potential undesirable incident. Before starting on the quantification, the participants should agree what they understand by the assessment criteria:

Likelihood

Minimal 1	Low 2	Medium 3	High 4	Very high 5
Once every 50 years or less	Once every 10 years or less	Once a year or less	Once a month or less	Once a week

Consequence

Grading	Human	Environment	Financial/material
E Very critical	May produce fatality/ies	Very prolonged, non-reversible damage	Shutdown of work >1 year.
D Critical	Permanent injury, may produce serious serious health damage/sickness	Prolonged damage. Long recovery time.	Shutdown of work 0.5-1 year.
C Dangerous	Serious personal injury	Minor damage. Long recovery time	Shutdown of work < 1 month
B Relatively safe	Injury that requires medical treatment	Minor damage. Short recovery time	Shutdown of work < 1week
A Safe	Injury that requires first aid	Insignificant damage. Short recovery time	Shutdown of work < 1day

The unit makes its own decision as to whether opting to fill in or not consequences for economy/materiel, for example if the unit is going to use particularly valuable equipment. It is up to the individual unit to choose the assessment criteria for this column.

Risk = Likelihood x Consequence

Please calculate the risk value for "Human", "Environment" and, if chosen, "Economy/materiel", separately.

About the column "Comments/status, suggested preventative and corrective measures":

Measures can impact on both likelihood and consequences. Prioritise measures that can prevent the incident from occurring; in other words, likelihood-reducing measures are to be prioritised above greater emergency preparedness, i.e. consequence-reducing measures.

MATRIX FOR RISK ASSESSMENTS at NTNU

CONSEQUENCE						
	Extremely serious	E1	E2	E3	E4	E5
	Serious	D1	D2	D3	D4	D5
	Moderate	C1	C2	C3	C4	C5
	Minor	B1	B2	B3	B4	B5
	Not significant	A1	A2	A3	A4	A5
		Very low	Low	Medium	High	Very high
		LIKELIHOOD				

Principle for acceptance criteria. Explanation of the colours used in the risk matrix.

Colour	Description
Red	Unacceptable risk. Measures must be taken to reduce the risk.
Yellow	Assessment range. Measures must be considered.
Green	Acceptable risk Measures can be considered based on other considerations.

NF

Standard Fan Nozzle

DESIGN FEATURES
- One-piece construction
- No internal parts
- Sizes for all applications
- Male connection

SPRAY CHARACTERISTICS
- High impact
- Uniform distribution with tapered edges for overlapping sprays
- Extra-wide angles available

Spray pattern: Fan and Straight Jet
Spray angles: 0° to 120°
Flow rates: 0.161 to 3430 l/min

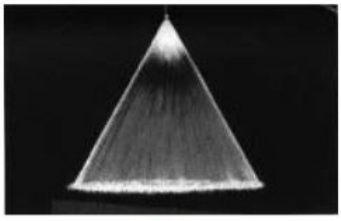

Fan 50°

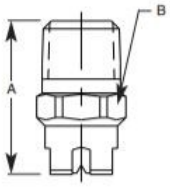

3/8" - 2" Metal

Call BETE to verify spray angle performance at operating pressures above 5 bar.

Dimensions are approximate. Check with BETE for critical dimension applications.

NF Flow Rates

Call BETE to verify spray angle performance at operating pressures above 5 bar.

Fan and Straight Jet, 0°, 15°, 30°, 50°, 65°, 80°, 90°, 110°, and 120° Spray Angles, 1/8" to 2" Pipe Sizes

Male Pipe Size	Nozzle Number	K Factor	LITERS PER MINUTE @ BAR 0.5 bar	0.7 bar	1 bar	2 bar	3 bar	5 bar	10 bar	30 bar	Equivalent Orifice Dia. (mm)
1/8	NF01	0.228	0.16	0.19	0.23	0.32	0.39	0.51	0.72	1.25	0.66
	NF015	0.342	0.24	0.29	0.34	0.48	0.59	0.76	1.08	1.87	0.79
or	NF02	0.455	0.32	0.38	0.46	0.64	0.79	1.02	1.44	2.49	0.91
	NF025	0.569	0.40	0.48	0.57	0.81	0.99	1.27	1.80	3.12	1.02
1/4	NF03	0.683	0.48	0.57	0.68	0.97	1.18	1.53	2.16	3.74	1.09
	NF04	0.911	0.64	0.76	0.91	1.29	1.58	2.04	2.88	4.99	1.32
	NF05	1.14	0.81	0.95	1.14	1.61	1.97	2.55	3.60	6.24	1.45
	NF06	1.37	0.97	1.14	1.37	1.93	2.37	3.06	4.33	7.49	1.57
	NF08	1.82	1.28	1.52	1.82	2.57	3.15	4.06	5.74	9.95	1.83
1/8	NF10	2.28	1.61	1.91	2.28	3.22	3.95	5.10	7.21	12.5	2.03
or	NF15	3.42	2.42	2.86	3.42	4.83	5.92	7.64	10.8	18.7	2.38
1/4	NF20	4.56	3.22	3.81	4.56	6.45	7.89	10.2	14.4	25.0	2.78
or	NF30	6.84	4.83	5.72	6.84	9.67	11.8	15.3	21.6	37.4	3.57
3/8	NF40	9.12	6.45	7.63	9.12	12.9	15.8	20.4	28.8	49.9	3.97
1/4	NF50	11.4	8.06	9.53	11.4	16.1	19.7	25.5	36.0	62.4	4.37
or	NF60	13.7	9.67	11.4	13.7	19.3	23.7	30.6	43.2	74.9	4.76
3/8	NF70	16.0	11.3	13.3	16.0	22.6	27.6	35.7	50.4	87.4	5.16
	NF60	13.7	9.67	11.4	13.7	19.3	23.7	30.6	43.2	74.9	4.76
3/8	NF70	16.0	11.3	13.3	16.0	22.6	27.6	35.7	50.4	87.4	5.16
or	NF80	18.2	12.9	15.3	18.2	25.8	31.6	40.8	57.7	99.9	5.56
1/2	NF90	20.5	14.5	17.2	20.5	29.0	35.5	45.9	64.9	112	5.95
	NF100	22.8	16.1	19.1	22.8	32.2	39.5	51.0	72.1	125	6.35
	NF120	27.3	19.3	22.9	27.3	38.7	47.4	61.1	86.5	150	6.75
1/2	NF150	34.2	24.2	28.6	34.2	48.3	59.2	76.4	108	187	7.54
	NF200	45.6	32.2	38.1	45.6	64.5	78.9	102	144	250	8.73
3/4	NF300	68.4	48.3	57.2	68.4	96.7	118	153	216	374	10.7
	NF400	91.2	64.5	76.3	91.2	129	158	204	288	499	12.7
1	NF400	91.2	64.5	76.3	91.2	129	158	204	288	499	12.7
	NF750	171	121	143	171	242	296	382	540	936	17.5
1 1/4	NF800	182	129	153	182	258	316	408	577	999	18.3
	NF1150	262	185	219	262	371	454	586	829	1440	21.8
1 1/2	NF1500	342	242	286	342	483	592	764	1080	1870	24.6
2	NF2250	513	362	429	513	725	890	1150	1620	2810	30.2

NF Dimensions

BSP or NPT

Pipe Size	Dim. for Metal Only (mm) A	B	Wt. (g) Metal	Plas.
1/8	22.2	11.1	28.4	7.09
1/4	27.0	14.3	42.5	10.6
3/8	31.8	17.5	56.7	14.2
1/2	38.1	22.2	85.1	28.4
3/4	44.5	28.6	170	42.5
1	55.6	34.9	227	56.7
1 1/4	63.5	44.5	340	85.1
1 1/2	76.2	50.8	567	142
2	88.9	63.5	1588	284

Flow Rate ($l/_{min}$) $= K\sqrt{bar}$ **Standard Materials: Brass, 303 Stainless Steel, 316 Stainless Steel, PVC, and PTFE**
(PTFE not available in nozzle numbers NF025 and under)

Spray angle performance varies with pressure. Contact BETE for specific data on critical applications.

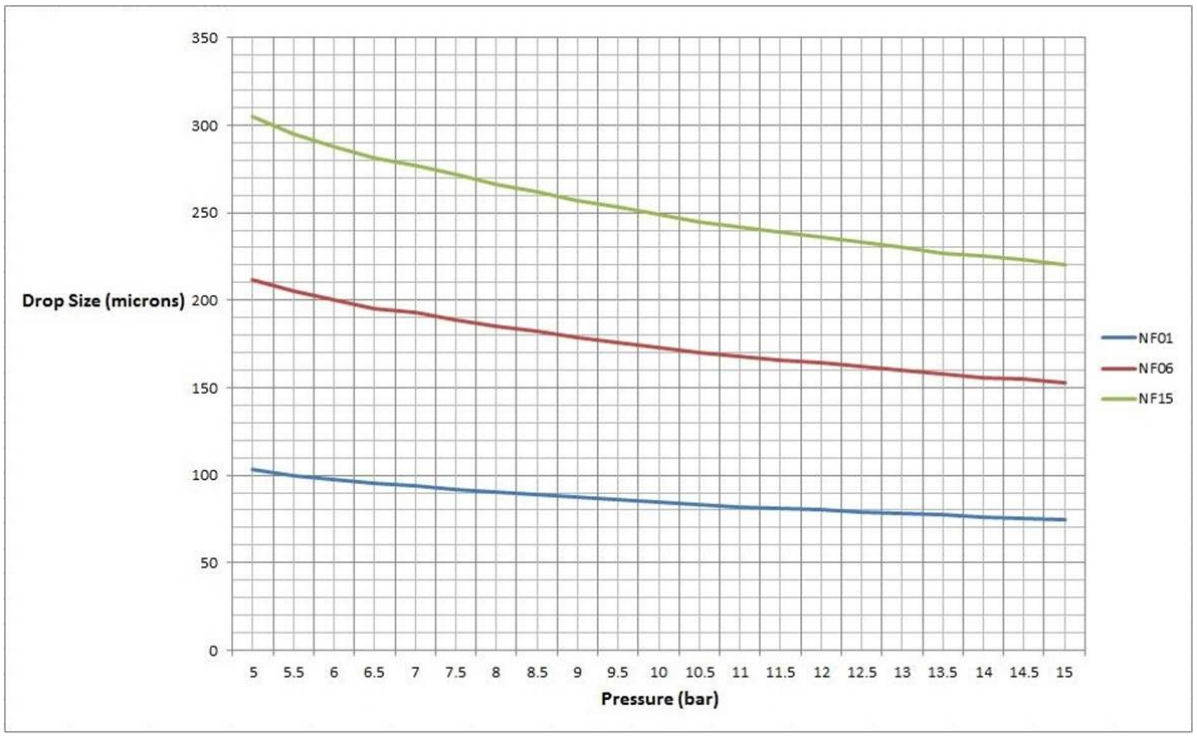

Figure B.0.1: Droplet size for NF01 and NF06 [30]

Appendix C – Progress plan